Journal of Human Genetics
(JHG-20-207 re-revised manuscript)

RNA sequencing-based microRNA expression signature in esophageal squamous cell carcinoma: oncogenic targets by antitumor *miR-143-5p* and *miR-143-3p* regulation

Masumi Wada[1], Yusuke Goto[2], Takako Tanaka[1], Reona Okada[2], Shogo Moriya[3], Tetsuya Idichi[1], Masahiro Noda[1], Ken Sasaki[1], Yoshiaki Kita[1], Hiroshi Kurahara[1], Kosei Maemura[1], Shoji Natsugoe[1], Naohiko Seki[2,#]

[1] Department of Digestive Surgery, Breast and Thyroid Surgery, Graduate School of Medical Sciences, Kagoshima University, Kagoshima, Japan
[2] Department of Functional Genomics, Chiba University Graduate School of Medicine, Chiba, Japan
[3] Department of Biochemistry and Genetics, Chiba University Graduate School of Medicine, Chiba, Japan

Running title: Molecular pathogenesis of ESCC based on the miRNA expression signature

[#]Correspondence to: Naohiko Seki, PhD
Associate Professor of Functional Genomics
Department of Functional Genomics
Chiba University Graduate School of Medicine
1-8-1 Inohana Chuo-ku, Chiba 260-8670, Japan
Tel: +81-43-226-2971
Fax: +81-43-227-3442
E-mail: naoseki@faculty.chiba-u.jp

Abstract:
Aberrantly expressed microRNAs (miRNAs) disrupt intracellular RNA networks and contribute to malignant transformation of cancer cells. Utilizing the latest RNA-sequencing technology, we newly created the miRNA expression signature of esophageal squamous cell carcinoma (ESCC). A total of 47 miRNAs were downregulated in ESCC tissues, and these miRNAs were candidates for antitumor miRNAs in ESCC cells. Analysis of the signature revealed that several passenger strands of miRNAs were significantly downregulated in ESCC, e.g., *miR-28-3p*, *miR-30a-3p*, *miR-30c-3p*, *miR-133a-3b*, *miR-139-3p*, *miR-143-5p*, and *miR-145-3p*. Recent studies indicate that some passenger strands of miRNAs closely involved in cancer pathogenesis. In this study, we focused on both strands of pre-*miR-143,* and investigated their antitumor roles and target oncogenes in ESCC. Ectopic expression of *miR-143-5p* and *miR-143-3p* significantly attenuated malignant phenotypes (e.g., proliferation, migration, and invasive abilities) in ESCC cell lines. We revealed that 6 genes (*HN1*, *HMGA2*, *NETO2*, *STMN1*, *TCF3* and *MET*) were putative targets of *miR-143-5p* regulation, and one gene (*KRT80*) was a putative target of *miR-143-3p* regulation in ESCC cells. Our ESCC miRNA signature and analysis strategy provided important insights into the molecular pathogenesis of ESCC.

Keywords:
microRNA; expression signature; esophageal squamous cell carcinoma; *miR-143-5p*; *miR-143-3p*, high-mobility group AT-hook 2 (HMGA2); Keratin 80 (KRT80)

Introduction

Esophageal cancer is divided histologically into two groups, i.e., esophageal squamous cell carcinoma (ESCC) and esophageal adenocarcinoma, and causes more than 500,000 deaths each year worldwide [1]. In Japan, more than 90% of the patients with esophageal cancer are diagnosed with ESCC, and ESCC is the 13th most common cause of cancer (approximately 23,000 new cases are diagnosed annually) [2]. Owing to the aggressive nature of ESCC, some patients exhibit local invasion and distant metastasis at the time of initial diagnosis [3-5]. Moreover, tumor recurrence frequently occurs after surgical resection [3-5]. Recently approved molecular targeted therapies have not been shown to be effective for the patients with metastasis and recurrence, and the prognosis of these patients remains poor [5,6]. Therefore, the discovery of novel therapeutic and diagnostic targets for ESCC based on advanced genomic analyses is urgently needed.

Human genome research has revealed that many noncoding RNA molecules are transcribed from the human genome. Additionally, these RNA molecules have been shown to play pivotal roles in various cellular processes under biological and pathological conditions [7]. Among these noncoding RNAs, microRNAs (miRNAs) are single-stranded RNAs, only 19–23 bases in length [8,9]. Notably, a single miRNA controls the expression of an extremely large number of RNA transcripts (protein-coding RNAs and noncoding RNAs) [8,9]. Aberrantly expressed miRNAs disrupt intracellular RNA networks and contribute to the malignant transformation of cancer cells [10,11].

We have been searching for miRNA-controlled molecular networks in cancer cells using aberrantly expressed miRNAs as indicators [12-16]. The first step is to select aberrantly expressed miRNAs in cancer cells. Creating our own miRNA expression signatures has been a major benefit for our miRNA-based cancer research. The latest RNA-sequencing technology is suitable for creating miRNA signatures, and our miRNA signatures indicate which miRNAs should be analyzed in each type of cancer [12-16]. Moreover, our RNA-sequencing based signatures have

demonstrated the importance of passenger strands of miRNAs derived from miRNA duplexes. According to the previous paradigm of miRNA biogenesis, passenger strands of miRNAs have no function in cells, whereas guide strands carry out miRNA functions [8,9]. Therefore, functional analysis of passenger strands of miRNAs in cancer cells and the search for target molecules regulated by these miRNAs have been rarely performed.

However, recent comprehensive database analysis has reported that both strands of miRNAs, e.g., *miR-30a-5p/-3p* and *miR-145-5p/-3p*, coordinately modulate oncogenic pathways across several types of cancers with prognostic effect [17]. This pan-cancer analysis is consistent with our previous our RNA-sequencing based signatures, which has revealed that several passenger strands of miRNAs are aberrantly expressed (down- or upregulated) in cancer tissues (e.g., *miR-143-5p*, *miR-144-5p*, *miR-145-3p*, *miR-150-3p*, and *miR-455-3p*) [12-16]. For example, downregulation of *miR-145-3p* (the passenger strand of the *miR-145* duplex) was detected in lung cancer, bladder cancer, prostate cancer, head and neck squamous cell carcinoma, and ESCC [13,18-22]. Ectopic expression of *miR-145-3p* markedly attenuates cancer cell malignant phenotypes in several types of cancers through targeting oncogenic genes [13,18-22]. Notably, overexpression of *miR-145-3p*-controlled oncogenes (e.g., *UHRF1*, *MTDH*, *MELK*, *NCAPG*, *BUB1*, *CDK1*, *MYO1B*, *LMNB2*, and *DHRS2*) was found to predict prognosis in patients with cancer [13,18-22]. Analysis of passenger strands of miRNAs should provide novel insights into cancer therapeutic targets and prognostic markers.

In this study, we newly created ESCC miRNA expression signature by RNA-sequencing. In total, 47 downregulated miRNAs were identified in ESCC. Interestingly, 4 miRNAs (*miR-143-5p*: passenger strand, *miR-143-3p*: guide strand, *miR-145-5p*: guide strand, and *miR-145-3p*: passenger strand) were significantly downregulated in ESCC tissues, and these miRNAs formed a miRNA cluster on human chromosome 5q32. We have recently revealed that both strands of the *miR-145* duplex act as antitumor miRNAs, and are closely involved in ESCC molecular pathogenesis [22]. Here,

we focused on both strands of *pre-miR-143* (*miR-143-5p* and *miR-143-3p*), and investigated the antitumor roles of these miRNAs in ESCC cells. Moreover, we revealed that 6 genes (*HN1*, *HMGA2*, *NETO2*, *STMN1*, *TCF3*, and *MET*) were putative targets of *miR-143-5p* regulation, and one gene (*KRT80*) was a putative target of *miR-143-3p* regulation in ESCC cells. The miRNA signature reported in this study would greatly contribute to the elucidation of the molecular pathogenesis of ESCC.

Materials and methods

Collection of clinical human ESCC specimens, esophageal epithelial specimens, and ESCC cell lines

In total, 8 specimens (4 ESCC tissues and 4 normal esophageal epithelial tissues) were analyzed by RNA-sequencing to create an ESCC miRNA signature (Supplementary Table 1). Thirty-four specimens (23 ESCC tissues and 11 normal esophageal epithelial tissues) were used to validate the expression statuses of miRNAs and target genes (Supplementary Table 1).

All specimens used in the study were obtained by surgical resection at Kagoshima University Hospital. All patients provided written informed consent for the use of their specimens. This study was approved by the Bioethics Committee of Kagoshima University (approval number: 28-65, February 10, 2015).

Two ESCC cell lines, TE-1 and TE-8 (American Type Culture Collection, Manassas, VA, USA), were used in this study.

Creation of the miRNA expression signature for ESCC based on RNA-sequencing

According to our previous studies [12-16], small RNA sequencing was performed to generate the miRNA expression signature of ESCC. Below is a brief description.

Total RNAs were extracted from 4 ESCC tissues and 4 normal tissues and subjected to RNA-sequencing. Total RNA of each sample was size-fractionated (20 to 30 nucleotides), and RNA

adaptors were ligated. Small RNAs ligated with adaptors were subjected to RT-PCR to produce sequencing libraries (approximately 120 nucleotide). Each cDNA library was sequenced by Genome Analyzer IIx (GAIIx) (Illumina Inc., CA, USA).

Sequence tags were produced by RNA-sequencing and high-quality clean reads (larger than 20 nucleotide) were mapped to the human genome using the SOAP program. Small RNA tags were aligned to the miRNA precursor/mature miRNA of corresponding species in miRBase release 22.1.

Assessment of differentially expressed miRNAs was determined with the edgeR program with the general linear model method. P-values are adjusted for multiple testing using the Benjamini and Hochberg method. The resulting sequence data was mined as previously reported [12-16].

Measurement of the expression statuses of miRNAs and mRNA in ESCC cells

RNA extraction from clinical tissues and cell lines was performed according to conventional methods [12-16]. Expression levels of miRNAs and genes were measured by TaqMan probes and primers according to conventional methods [12-16]. The reagents used in this study are listed in Supplementary Table 2.

Functional assays by ectopic expression of miRNAs, small interfering RNAs (siRNAs), and plasmid vectors in ESCC cells

Transfection procedures for miRNAs, genes, and plasmid vectors were described in our previous studies [12-16].

Functional assays using cancer cells (cell proliferation, migration, and invasion) were performed according to conventional methods [12-16]. The reagents used are listed in Supplementary Table 2.

Identification of putative targets regulated by *miR-143-5p* and *miR-143-3p* in ESCC cells

Supplementary Fig.1 shows the strategy for searching for candidate oncogenic genes controlled by *miR-143-5p* and *miR-143-*

3p in ESCC cells. We downloaded putative 3'-UTR target sites for each microRNAs from TargetScan database release 7.2 (http://www.targetscan.org/vert_72/). As for comparison of mRNA between cancer vs. normal tissues, we downloaded data from The Cancer Omics Atlas (https://tcoa.cpu.edu.cn/index.php). As for the mRNA expression data for putative 40 genes (31 genes were regulated by *miR-143-5p*, and 9 genes were regulated by *miR-143-3p*), we downloaded data (HiSeq V2 RSEM) of TCGA-ESCA from https://xena.ucsc.edu/.

Direct control of *miR-143-5p* or *miR-143-5p* by dual-luciferase reporter assays

The vectors used for this analysis were constructed in accordance with our previous studies [12-16]. Figure S2 shows the sequences incorporated into the vectors. The analysis procedure was performed according to our previous studies [12-16]. The reagents used are listed in Supplementary Table 2.

Western blotting and immunohistochemistry

The antibodies used in this study are listed in Supplementary Table 2. Whole Western blotting images following miRNAs (*miR-143-5p* or *miR-143-3p*) or siRNA (si*HMGA2* or si*KRT80*) transfection into ESCC cell lines were shown in Supplementary Figures.

Statistical analysis

Statistical analyses were performed with GraphPad Prism 7 (GraphPad Software, La Jolla, CA, USA) and JMP Pro 14 (SAS Institute Inc., Cary, NC, USA). Mann–Whitney U tests were performed to determine the significance of differences between the two groups. One-way analysis of variance and Tukey tests for post-hoc analysis were applied for multiple groups.

Results

Generation of the miRNA expression signature of ESCC by RNA-sequencing

Eight cDNA libraries (4 ESCC tissues and 4 normal esophageal epithelial tissues) were analyzed by RNA-sequencing. In this analysis, we obtained between 27,864,484 and 33,253,231 total sequence reads (Supplementary Table 3). After a trimming procedure, between 6,314,266 and 26,123,671 reads were successfully mapped on the human genome. Among these read sequences, we identified human small RNAs (Supplementary Table 3).

In total, 47 downregulated miRNAs were identified as ESCC-associated miRNAs (Table 1). Notably, analysis of our ESCC signature revealed that 8 miRNA duplexes (guide strand and passenger strand pairs, e.g., *miR-133a*, *miR-145*, *miR-143*, *miR-139*, *miR-30a*, *miR-28*, *miR-378a*, and *miR-30c*) derived from pre-miRNAs were downregulated in ESCC tissues (Table 1).

The clinical features of the specimens using in this study are summarized in Supplementary Table 1.

Antitumor functions of *miR-143-5p* and *miR-143-3p* in ESCC by ectopic expression assays

Some miRNAs are located close together in the human genome (forming miRNA clusters). Among these miRNA clusters, *pre-miR-145* and *pre-miR-143* are mapped to human chromosome 5q32. Our signature showed that 4 miRNAs (*miR-143-5p*, *miR-143-3p*, *miR-145-5p*, and *miR-145-3p*) were significantly downregulated in ESCC tissues. Our previous study showed that *miR-145-5p* and *miR-145-3p* acted as antitumor miRNAs in ESCC cells through targeting several oncogenic genes [22]. In this study, we investigated the functional significance and their controlled oncogenic genes of both strands of *miR-143*-duplex (*miR-143-5p*: the passenger strand and *miR-143-3p*: the guide strand) in ESCC cells.

To confirm the validity of the ESCC signature, we measured the expression levels of *miR-143-5p* and *miR-143-3p* in clinical specimens (23 ESCC specimens and 11 normal esophageal epithelial specimens). Expression levels of *miR-143-5p* ($p < 0.0001$) and *miR-143-3p* ($p = 0.0173$) were significantly reduced in ESCC tissues compared with those in normal esophageal epithelial

tissues (Fig. 1A). The expression levels of these miRNAs in the two cell lines (TE-1 and TE-8) were lower than those in normal esophageal epithelial tissues (Fig. 1A). There was a positive correlation between the expression levels of the two miRNAs by Spearman's rank analysis (r = 0.657, p < 0.0001; Fig. 1B).

To investigate the antitumor functions of *miR-143-5p* and *miR-143-3p* in ESCC cells, we performed ectopic expression assays. The experiment was performed by a transient transfection method using mature types of miRNAs, *miR-143-5p* (ggugcagugcugcaucucuggu) or *miR-143-3p* (ugagaugaagcacuguagcuc).

Cell proliferation ability was not blocked by *miR-143-5p* or *miR-143-3p* transfection into ESCC cell lines (Fig. 1C). In contrast, cell migration and invasive abilities were significantly attenuated by *miR-143-5p* and *miR-143-3p* transfection into ESCC cell lines (Figs. 1D and 1E). Typical images of migration and invasion assays are shown in Supplemental Figure 2.

Screening of putative oncogenic targets by *miR-143-5p* and *miR-143-3p* regulation in ESCC cells

To identify the putative oncogenic targets of *miR-143-5p* regulation in ESCC cells, we assessed 3 datasets, i.e., TargetScan database (to identify putative targets of *miR-143-5p* by *in silico*) and gene expression data (genes downregulated in *miR-143-5p*-transfected ESCC cells and genes upregulated in ESCC clinical specimens). Our screening strategy of *miR-143-5p* or *miR-143-3p* targets is shown in Supplementary Fig. 1. A total of 31 genes were putative targets of *miR-143-5p* regulation in ESCC cells (Table 2A). Among these genes, 6 genes (*HN1*, *HMGA2*, *NETO2*, *STMN1*, *TCF3*, and *MET*) were upregulated in ESCC clinical specimens (Fig. 2).

Using a similar strategy, a total of 9 genes were identified as *miR-143-3p* regulation. Among these targets, we identified *KRT80* as an oncogenic target by *miR-143-3p* regulation in ESCC cells (Table 2B and Fig. 2).

The expression patterns of the remaining genes are shown in

Supplemental Fig. 3A-3C.

Direct regulation of *HMGA2* by *miR-143-5p* and *KRT80* by *miR-143-3p* in ESCC cells

By focusing on passenger strand and ESCC clinical specimen, *HMGA2* was the most upregulated gene among 6 putative genes regulated by *miR-143-5p* in ESCC (Log_2 Fold change; *HMGA2*: 3.19; *STMN1*: 2.16; *NETO2*: 1.77; *HN1*: 1.75; *TCF3*: 1.21 and *MET*: 1.1). In this regard, we focused on *HMGA2* for further analysis since *HMGA2* could have an important role in ESCC progression.

First, we analyzed the direct regulation of *HMGA2*. Expression levels of *HMGA2*/HMGA2 (mRNA and protein) were reduced by *miR-143-5p* transfection in ESCC cells (Supplementary Figs. 4A and 4B).

Accordingly, we then examined whether *miR-143-5p* bound directly to the 3′-untranslated region (3′-UTR) of *HMGA2* by dual-luciferase reporter assays. Using the TargetScan database, three putative *miR-143-5p* binding sites were identified in the 3′-UTR of *HMGA2* (Supplementary Figs. 4C-4E). Our data showed that luminescence intensities were significantly reduced by cotransfection of *miR-143-5p* and vectors carrying *miR-143-5p* binding sites in the 3′-UTR of *HMGA2* (Supplementary Figs. 4C-4E). In contrast, cotransfection of *miR-145-5p* and vectors without *miR-143-5p* binding sites (deleted *miR-143-5p* binding sites) did not show reduced luminescence intensities (Supplementary Figs. 4C-4E). These data indicated that *miR-143-5p* could bind to three binding sites in the 3′-UTR of *HMGA2* in ESCC cells.

Furthermore, we analyzed the suppression of *KRT80* by *miR-143-3p* in ESCC cells. Expression levels of *KRT80*/KRT80 (mRNA and protein) were reduced by *miR-143-3p* transfection in ESCC cells (Supplementary Figs. 5A and 5B). TargetScan database showed that one putative *miR-143-3p* binding site was identified in the 3′-UTR of *KRT80* (Supplementary Fig. 5C). The luminescence intensities were significantly reduced by cotransfection of *miR-143-3p* and vectors carrying *miR-143-3p* binding site in the 3′-

UTR of *KRT80* (Supplementary Fig. 5C). Our data indicated that the expression of *KRT80* was directly regulated by *miR-143-3p* in ESCC cells.

We also analyzed the regulation of 5 genes (*HN1*, *NETO2*, *STMN1*, *TCF3* and *MET*) by *miR-143-5p* in ESCC cells (Supplementary Fig. 6).

Overexpression of HMGA2 and KRT80 in ESCC clinical specimens

To confirm HMGA2 protein expression in clinical specimens, we performed immunostaining for HMGA2. Overexpression of HMGA2 was detected in cancer lesions (Fig. 3 Upper).

The expression of *HMGA2* was significantly upregulated in ESCC tissues (Supplemental Fig. 7). The expression of *miR-143-5p* was negatively correlated with the expression of *HMGA2* in ESCC clinical specimens (Supplemental Fig. 7).

Immunostaining of KRT80 was performed using ESCC clinical specimens. Overexpression of KRT80 was detected in cancer lesions (Fig. 3 Lower).

Effects of *HMGA2* knockdown in ESCC cells

HMGA2/HMGA2 overexpression in ESCC clinical specimens prompted us to further analyze functional roles of HMGA2 in ESCC cells. In this regard, we performed *HMGA2* knockdown assays using two types of siRNAs. The expression levels of both *HMGA2* mRNA and HMGA2 protein were markedly reduced by si*HMGA2*-1 and si*HMGA2*-2 in the two cell lines (Figs. 4A and 4B). Whole Western blotting images were shown in Supplemental Figure 8.

By suppressing *HMGA2* expression, malignant phenotypes (e.g., cell proliferation, migration, and invasive abilities) in ESCC cells were significantly blocked (Figs. 4C-4E). These data suggested that aberrant expression of *HMGA2* promoted cancer-related phenotypes in ESCC cells.

Effects of *KRT80* knockdown in ESCC cells

To address the oncogenic function of *KRT80* in ESCC cells, we performed knockdown assay using si*KRT80* in ESCC cells.

We confirmed that the *KRT80*/KRT80 expressions in ESCC cells were suppressed by the transfection of two types of siRNAs (Figs. 4F and 4G). Whole Western blotting images were shown in Supplemental Figure 9. By suppressing *KRT80* expression, cancer cell proliferation, migration, and invasive abilities were significantly blocked in ESCC cells (Figs. 4H-4J). These data indicated that aberrant expression of *KRT80* enhanced malignant phenotypes of ESCC cells.

In this study, ectopic expression of *miR-143-5p* and *miR-143-3p* had not affected cell proliferation in ESCC cells. In contrast to this, knockdown of *HMGA2* or *KRT80* affected cell proliferation in ESCC cells. Due to the unique nature of miRNA, a single miRNA controls a vast number of RNA transcripts in normal and disease cells. In ESCC cells, *miR-143-5p* and *miR-143-3p* may not only control genes that promote cell growth, but may also affect genes that suppress cell growth. Another hypothesis is that siRNA is more effective than miRNA in suppressing *HMGA2* or *KRT80* in ESCC cells. It is necessary to comprehensively elucidate the molecular network controlled by *miR-143-5p* and *miR-143-3p* in ESCC cells.

Downstream genes affected by knockdown of *HMGA2* in ESCC cells

We performed genome-wide gene expression analyses by using si*HMGA2* transfected ESCC cells (TE-8 cells). Genes significantly downregulated by silencing of *HMGA2* are listed in Supplemental Table 4. Genecodis (https://genecodis.genyo.es/) database analyses revealed that several biological pathways were affected by *HMGA2* expression, e.g., "DNA replication", "Cell cycle", "Mismatch repair", and "Nucleotide excision repair" (Supplemental Table 4). The gene expression data were deposited in GEO database (accession number: GSE143822).

Discussion

ESCC is associated with a high mortality rate owing to frequent recurrence and metastasis after primary treatment [3-6]. No

molecular-targeted drugs have been developed for the treatment of ESCC, and novel treatment options for patients with advanced ESCC are urgently needed. Thus, in our laboratory, we are developing miRNA-based approaches to identify therapeutic targets for ESCC [22-25]. We previously produced a miRNA expression signature for ESCC using a polymerase chain reaction (PCR)-based array [23]. According to this signature, we identified antitumor miRNAs and their direct oncogenic target genes in ESCC cells, e.g., *miR-133a* (targeting *FSCN1*), *miR-133b* (targeting *FSCN1*), *miR-145-5p* (targeting *FSCN1*), *miR-375* (targeting *MMP13*), and *miR-150-5p* (targeting *SPOCK1*) [22-25].

Currently available high-throughput RNA-sequencing technologies are suitable for the construction of miRNA expression signatures for human cancers. Our RNA-sequencing-based miRNA signatures revealed that some passenger strands of miRNAs are significantly up- or downregulated in cancer tissues [12-16]. Based on these signatures, we sequentially identified antitumor miRNAs (passenger strands of miRNAs) and their controlled novel oncogenes and oncogenic pathways, e.g., *miR-150-3p* (targeting *ITGA3*, *ITGA6*, and *TNC*), *miR-216b-3p* (targeting *FOXQ1*), *miR-199a/b-3p* (targeting *NCAPH*), and *miR-101-5p* (targeting *GINS1*) [12-16]. Recent pan-cancer miRNA signature analysis with RNA interference and CRISPR screen showed that both the passenger strand and the guide strand simultaneously function to modulate cancer progression, which is consistent with our previous and current studies [17].

Analysis of the ESCC miRNA signature in this study revealed that all members of the *miR-143/miR-145* cluster were downregulated. Many studies have shown that *miR-143-3p* (the guide strand) and *miR-145-5p* (the guide strand) are frequently downregulated in several cancers, including ESCC, and that both miRNAs function as tumor suppressors [26-31]. Notably, their promoter region has a p53 response element, and their expression levels are controlled by the activation of p53 in physiological and pathological conditions [32]. Therefore, the genes controlled by the *miR-143/miR-145* cluster are important for p53-

mediated tumor-suppressive mechanisms. More recently, we showed that *miR-145-3p* had antitumor roles (e.g., blocking of cell proliferation, migration, and invasion and induction of apoptosis) in ESCC cells and that *DHRS2* and *MYO1B* were directly regulated by *miR-145-3p* in ESCC cells [22]. Aberrant expression of *DHRS2* and *MYO1B* was detected in ESCC clinical specimens, and overexpression of these genes enhanced malignant phenotypes in ESCC cells [22]. Our continuous studies of *miR-145-3p* revealed that *miR-145-3p* controlled molecular pathways that are closely involved in molecular pathogenesis of human cancers, e.g., bladder cancer, prostate cancer, lung cancer, and head and neck squamous cell carcinoma [13, 18-21].

In the current study, we focused on *miR-143-5p* (the passenger strand of the *miR-143* duplex), and ectopic expression assays revealed that this miRNA had antitumor functions. Recent studies have shown that *miR-143-5p* acts as an antitumor miRNA in several cancers by targeting various oncogenes, e.g., gastric cancer (targeting *COX-1*), gallbladder cancer (targeting *HIF-1α* and lung cancer (targeting *MCM4*) [33-35]. Moreover, aberrant expression of long noncoding RNAs (lncRNAs) has been shown to contribute to ESCC by promoting metastasis and drug resistance [36,37]. Several lncRNAs, including *ZEB2-AS1* (gastric cancer), *TCONS-00026907* (cervical cancer), and *LINC01207* (pancreatic cancer), are overexpressed in cancer cells and function as miRNAs sponges to negatively regulate antitumor *miR-143-5p* expression [38-40]. For example, in esophageal cancer, *HAGLR* suppresses *miR-143-5p* and increases the expression of *LAMP3* to promote aggressive phenotypes in cancer cells [41].

Searching for oncogenic targets controlled by antitumor *miR-145-3p* will contribute to elucidating the molecular pathogenesis of ESCC. Our current study identified 6 genes (*HN1*, *HMGA2*, *NETO2*, *STMN1*, *TCF3*, and *MET*) as putative oncogenic targets regulated by *miR-143-5p* in ESCC cells. Likewise, *KRT80* was detected as the *miR-143-3p* target in ESCC cells. Detailed functional analysis of these genes will lead to elucidation of the molecular mechanisms of esophageal cancer.

In this study, we focused on *HMGA2* (encodes high mobility group A2) as a target by *miR-143-5p* regulation. Our recent study of lung adenocarcinoma listed that *HMGA2* was a candidate target for controlled by *miR-143-5p* [35]. HMGA2 is a member of the nonhistone chromosomal high-mobility group protein family. This protein has three AT-hooks that can bind to AT-rich regions of DNA and assist with transcriptional activation by altering chromatin architecture [42-44]. Our functional assays showed that aberrant expression of *HMGA2* enhanced ESCC cell malignant phenotypes. Notably, aberrant expression of *HMGA2* has been reported in various cancers, including ESCC, and its expression contributes to cancer cell development, metastasis, and drug resistance [45,46].

Previous studies showed that the expression of HMGA2 affected a wide range of biological process, e.g., cell cycle, DNA damage repair, epithelial-mesenchymal transition, and apoptosis [45]. Our present data of *MHGA2* knockdown ESCC cells showed that several biological pathways were affected by *HMGA2* expression, e.g., "DNA replication", "Cell cycle", "Mismatch repair", and "Nucleotide excision repair". Aberrant expression of DNA-repair genes contributed to drug resistance in cancer cells [45]. It has been shown that overexpression of *HMGA2* may be involved in drug resistance in cancer cells. In fact, the TCGA database analyses revealed that high expression of *HMGA2* has an impact on prognosis with cancer patients, e.g., head and neck cancer, renal cell carcinoma, pancreatic adenocarcinoma and sarcoma. In addition, High expression of *HMGA2* is associated with a poor prognosis in patients with ESCC [47-49]. These findings suggest that *HMGA2* may be a therapeutic target for ESCC.

Furthermore, our present study demonstrated that aberrant expression of *KRT80* was detected in ESCC clinical specimens, and its overexpression closely contributed to ESCC malignant phenotypes. This is the first report that *KRT80* has an oncogene function in ESCC cells. A previous study in colon cancer showed that expression of *KRT80* was an independent prognostic biomarker

of this disease, and its expression promoted colon cancer migration and invasion [50]. Detailed functional analysis of *KRT80* will be helpful in understanding the novel molecular pathogenesis of ESCC cells.

In conclusion, we created a novel miRNA expression signature for ESCC using RNA-sequencing analysis. This signature indicated that 47 miRNAs were downregulated in ESCC tissues. A major advantage of this signature is that it contained multiple passenger strands of miRNAs derived from miRNA duplexes, e.g., *miR-28-3p*, *miR-30a-3p*, *miR-30c-3p*, *miR-133a-3b*, *miR-139-3p*, *miR-143-5p*, and *miR-145-3p*. The involvement of passenger strands of miRNA in the molecular pathogenesis of ESCC is a new concept. We revealed that *miR-143-5p* had antitumor functions and a total of 6 genes (*HN1*, *HMGA2*, *NETO2*, *STMN1*, *TCF3*, and *MET*) as putative oncogenic targets regulated by *miR-143-5p*, and one target gene (*KRT80*) regulated by *miR-143-3p* in ESCC cells. Overexpression of *HMGA2* and *KRT80* closely involved in the malignant transformation of ESCC. Our ESCC miRNA signature and antitumor miRNA-based analyses will provide important insights into the molecular pathogenesis of ESCC.

Acknowledgements

This study was supported by KAKENHI grants (grant nos. 17H04285, 18K08626, 18K09338, 18K16322 and 19K09077).

Conflicts of Interest

The authors declare no conflicts of interest.

References

1. Bray F, Ferlay J, Soerjomataram I, Siegel RL, Torre LA, Jemal A. Global cancer statistics 2018: GLOBOCAN estimates of incidence and mortality worldwide for 36 cancers in 185 countries. CA Cancer J Clin. 2018;68:394-424.
2. Lin Y, Totsuka Y, He Y, Kikuchi S, Qiao Y, Ueda J, et al. Epidemiology of esophageal cancer in Japan and China. J Epidemiol. 2013;23:233-42.
3. Pennathur A, Gibson MK, Jobe BA, Luketich JD. Oesophageal carcinoma. Lancet. 2013;381:400-12.
4. Watanabe M, Otake R, Kozuki R, Toihata T, Takahashi K, Okamura A, et al. Recent progress in multidisciplinary treatment for patients with esophageal cancer. Surg Today. 2020;50:12-20.
5. Tanaka Y, Yoshida K, Suetsugu T, Imai T, Matsuhashi N, Yamaguchi K. Recent advancements in esophageal cancer treatment in Japan. Ann Gastroenterol Surg. 2018;2:253-65.
6. Hirano H, Kato K. Systemic treatment of advanced esophageal squamous cell carcinoma: chemotherapy, molecular-targeting therapy and immunotherapy. Jpn J Clin Oncol. 2019;49:412-20.
7. Anfossi S, Babayan A, Pantel K, Calin GA. Clinical utility of circulating non-coding RNAs - an update. Nat Rev Clin Oncol. 2018;15:541-63.
8. Ha M, Kim VN. Regulation of microRNA biogenesis. Nat Rev Mol Cell Biol. 2014;15:509-24.
9. Gebert LFR, MacRae IJ. Regulation of microRNA function in animals. Nat Rev Mol Cell Biol. 2019;20:21-37.
10. Lin S, Gregory RI. MicroRNA biogenesis pathways in cancer. Nat Rev Cancer. 2015;15:321-33.
11. Rupaimoole R, Slack FJ. MicroRNA therapeutics: towards a new era for the management of cancer and other diseases. Nat Rev Drug Discov. 2017;16:203-22.
12. Koshizuka K, Nohata N, Hanazawa T, Kikkawa N, Arai T, Okato A, et al. Deep sequencing-based microRNA expression signatures in head and neck squamous cell carcinoma: dual

strands of pre-miR-150 as antitumor miRNAs. Oncotarget. 2017;8:30288-304.
13. Goto Y, Kurozumi A, Arai T, Nohata N, Kojima S, Okato A, et al. Impact of novel miR-145-3p regulatory networks on survival in patients with castration-resistant prostate cancer. Br J Cancer. 2017;117:409-20.
14. Yonemori K, Seki N, Idichi T, Kurahara H, Osako Y, Koshizuka K, et al. The microRNA expression signature of pancreatic ductal adenocarcinoma by RNA sequencing: anti-tumour functions of the microRNA-216 cluster. Oncotarget. 2017;8:70097-115.
15. Arai T, Kojima S, Yamada Y, Sugawara S, Kato M, Yamazaki K, et al. Micro-ribonucleic acid expression signature of metastatic castration-resistant prostate cancer: Regulation of NCAPH by antitumor miR-199a/b-3p. Int J Urol. 2019;26:506-20.
16. Toda H, Seki N, Kurozumi S, Shinden Y, Yamada Y, Nohata N, et al. RNA-sequence-based microRNA expression signature in breast cancer: tumor-suppressive miR-101-5p regulates molecular pathogenesis. Mol Oncol. 2020;14:426-46.
17. Mitra R, Adams CM, Jiang W, Greenawalt E, Eischen CM. Pan-cancer analysis reveals cooperativity of bothstrands of microRNA that regulate tumorigenesis and patient survival. Nat Commun. 2020;11:968.
18. Matsushita R, Yoshino H, Enokida H, Goto Y, Miyamoto K, Yonemori M, et al. Regulation of UHRF1 by dual-strand tumor-suppressor microRNA-145 (miR-145-5p and miR-145-3p): Inhibition of bladder cancer cell aggressiveness. Oncotarget. 2016;7:28460-87.
19. Mataki H, Seki N, Mizuno K, Nohata N, Kamikawaji K, Kumamoto T, et al. Dual-strand tumor-suppressor microRNA-145 (miR-145-5p and miR-145-3p) coordinately targeted MTDH in lung squamous cell carcinoma. Oncotarget. 2016;7:72084-98.
20. Yamada Y, Koshizuka K, Hanazawa T, Kikkawa N, Okato A, Idichi T, et al. Passenger strand of miR-145-3p acts as a

tumor-suppressor by targeting MYO1B in head and neck squamous cell carcinoma. Int J Oncol. 2018;52:166-78.
21. Misono S, Seki N, Mizuno K, Yamada Y, Uchida A, Arai T, et al. Dual strands of the miR-145 duplex (miR-145-5p and miR-145-3p) regulate oncogenes in lung adenocarcinoma pathogenesis. J Hum Genet. 2018;63:1015-28.
22. Shimonosono M, Idichi T, Seki N, Yamada Y, Arai T, Arigami T, et al. Molecular pathogenesis of esophageal squamous cell carcinoma: Identification of the antitumor effects of miR1453p on gene regulation. Int J Oncol. 2019;54:673-88.
23. Kano M, Seki N, Kikkawa N, Fujimura L, Hoshino I, Akutsu Y, et al. miR-145, miR-133a and miR-133b: Tumor-suppressive miRNAs target FSCN1 in esophageal squamous cell carcinoma. Int J Cancer. 2010;127:2804-14.
24. Osako Y, Seki N, Kita Y, Yonemori K, Koshizuka K, Kurozumi A, et al. Regulation of MMP13 by antitumor microRNA-375 markedly inhibits cancer cell migration and invasion in esophageal squamous cell carcinoma. Int J Oncol. 2016;49:2255-64.
25. Osako Y, Seki N, Koshizuka K, Okato A, Idichi T, Arai T, et al. Regulation of SPOCK1 by dual strands of pre-miR-150 inhibit cancer cell migration and invasion in esophageal squamous cell carcinoma. J Hum Genet. 2017;62:935-44.
26. Ni Y, Meng L, Wang L, Dong W, Shen H, Wang G, et al. MicroRNA-143 functions as a tumor suppressor in human esophageal squamous cell carcinoma. Gene. 2013;517:197-204.
27. Liu R, Liao J, Yang M, Sheng J, Yang H, Wang Y, et al. The cluster of miR-143 and miR-145 affects the risk for esophageal squamous cell carcinoma through co-regulating fascin homolog 1. PLoS One. 2012;7:e33987.
28. Zeinali T, Mansoori B, Mohammadi A, Baradaran B. Regulatory mechanisms of miR-145 expression and the importance of its function in cancer metastasis. Biomed Pharmacother. 2019;109:195-207.
29. Ye D, Shen Z, Zhou S. Function of microRNA-145 and

mechanisms underlying its role in malignant tumor diagnosis and treatment. Cancer Manag Res. 2019;11:969-79.
30. Xu WX, Liu Z, Deng F, Wang DD, Li XW, Tian T, et al. MiR-145: a potential biomarker of cancer migration and invasion. Am J Transl Res. 2019;11:6739-53.
31. Hu M, Zhang Q, Tian XH, Wang JL, Niu YX, Li G. lncRNA CCAT1 is a biomarker for the proliferation and drug resistance of esophageal cancer via the miR-143/PLK1/BUBR1 axis. Mol Carcinog. 2019;58:2207-17.
32. Sachdeva M, Zhu S, Wu F, Wu H, Walia V, Kumar S, et al. p53 represses c-Myc through induction of the tumor suppressor miR-145. Proc Natl Acad Sci U S A. 2009;106:3207-12.
33. Wu XL, Cheng B, Li PY, Huang HJ, Zhao Q, Dan ZL, et al. MicroRNA-143 suppresses gastric cancer cell growth and induces apoptosis by targeting COX-2. World J Gastroenterol. 2013;19:7758-65.
34. He M, Zhan M, Chen W, Xu S, Long M, Shen H, et al. MiR-143-5p Deficiency Triggers EMT and Metastasis by Targeting HIF-1alpha in Gallbladder Cancer. Cell Physiol Biochem. 2017;42:2078-92.
35. Sanada H, Seki N, Mizuno K, Misono S, Uchida A, Yamada Y, et al. Involvement of Dual Strands of miR-143 (miR-143-5p and miR-143-3p) and Their Target Oncogenes in the Molecular Pathogenesis of Lung Adenocarcinoma. Int J Mol Sci. 2019;20:4482.
36. Talebi A, Masoodi M, Mirzaei A, Mehrad-Majd H, Azizpour M, Akbari A. Biological and clinical relevance of metastasis-associated long noncoding RNAs in esophageal squamous cell carcinoma: A systematic review. J Cell Physiol. 2020;235:848-68.
37. Sugihara H, Ishimoto T, Miyake K, Izumi D, Baba Y, Yoshida N, et al. Noncoding RNA Expression Aberration Is Associated with Cancer Progression and Is a Potential Biomarker in Esophageal Squamous Cell Carcinoma. Int J Mol Sci. 2015;16:27824-34.

38. Wu F, Gao H, Liu K, Gao B, Ren H, Li Z, et al. The lncRNA ZEB2-AS1 is upregulated in gastric cancer and affects cell proliferation and invasion via miR-143-5p/HIF-1alpha axis. Onco Targets Ther. 2019;12:657-67.
39. Liu C, Wang JO, Zhou WY, Chang XY, Zhang MM, Zhang Y, et al. Long non-coding RNA LINC01207 silencing suppresses AGR2 expression to facilitate autophagy and apoptosis of pancreatic cancer cells by sponging miR-143-5p. Mol Cell Endocrinol. 2019;493:110424.
40. Jin X, Chen X, Hu Y, Ying F, Zou R, Lin F, et al. LncRNA-TCONS_00026907 is involved in the progression and prognosis of cervical cancer through inhibiting miR-143-5p. Cancer medicine. 2017;6:1409-23.
41. Yang C, Shen S, Zheng X, Ye K, Sun Y, Lu Y, et al. Long noncoding RNA HAGLR acts as a microRNA-143-5p sponge to regulate epithelial-mesenchymal transition and metastatic potential in esophageal cancer by regulating LAMP3. FASEB J. 2019;33:10490-504.
42. Young AR, Narita M. Oncogenic HMGA2: short or small? Genes Dev. 2007;21:1005-9.
43. Hammond SM, Sharpless NE. HMGA2, microRNAs, and stem cell aging. Cell. 2008;135:1013-6.
44. Pfannkuche K, Summer H, Li O, Hescheler J, Droge P. The high mobility group protein HMGA2: a co-regulator of chromatin structure and pluripotency in stem cells? Stem Cell Rev Rep. 2009;5:224-30.
45. Fedele M, Palmieri D, Fusco A. HMGA2: A pituitary tumour subtype-specific oncogene? Mol Cell Endocrinol. 2010;326:19-24.
46. Zhang S, Mo Q, Wang X. Oncological role of HMGA2 (Review). Int J Oncol. 2019;55:775-88.
47. Palumbo A, Jr., Da Costa NM, Esposito F, De Martino M, D'Angelo D, de Sousa VP, et al. HMGA2 overexpression plays a critical role in the progression of esophageal squamous carcinoma. Oncotarget. 2016;7:25872-84.
48. Palumbo Junior A, Da Costa NM, Esposito F, Fusco A, Pinto

LF. High Mobility Group A proteins in esophageal carcinomas. Cell Cycle. 2016;15:2410-3.

49. Wei R, Shang Z, Leng J, Cui L. Increased expression of high-mobility group A2: A novel independent indicator of poor prognosis in patients with esophageal squamous cell carcinoma. J Cancer Res Ther. 2016;12:1291-97.

50. Li C, Liu X, Liu Y, Liu X, Wang R, Liao J, et al. Keratin 80 Promotes Migration and Invasion of Colorectal Carcinoma by Interacting With PRKDC via Activating the AKT Pathway. Cell Death. Dis.2018;9:1009.

Figure legends

Figure 1: Antitumor roles of *miR-143-5p* and *miR-143-3p* in ESCC cells.

(A) Expression of *miR-143-5p* and *miR-143-3p* in ESCC clinical specimens and cells lines (TE-1 and TE-8). Data were normalized to the expression of *U6*. (B) Spearman's rank tests showed positive correlations between expression levels of *miR-143-5p* and *miR-143-3p* in clinical specimens. (C-E) Functional assays of cell proliferation, migration, and invasion following ectopic expression of *miR-143-5p* and *miR-143-3p* in ESCC cell lines (TE-1 and TE-8). (C) Cell proliferation was assessed using XTT assays. Data were collected 72 h after miRNA transfection (*$p < 0.0001$). (D) Cell migration was assessed with a membrane culture system. Data were collected 48 h after seeding the cells into the chambers (*$p < 0.0001$). (E) Cell invasion was determined 48 h after seeding miRNA-transfected cells into chambers using Matrigel invasion assays (*$p < 0.0001$).

Figure 2: Expression levels of target genes by *miR-143-5p* or *miR-143-3p* regulation in ESCC specimens by TCGA analyses

As for putative targets of *miR-143-5p*, mRNA expression of 6 genes (*HN1*, *HMGA2*, *NETO2*, *STMN1*, *TCF3* and *MET*) were significantly upregulated in ESCC clinical specimens (n = 185) compared to normal specimens (n = 11). As for putative targets of *miR-143-3p*, mRNA expression of *KRT80* was significantly upregulated in ESCC clinical specimens (n = 185) compared to normal specimens (n = 11) (Mann-Whitney test).
The expression data were downloaded from http://xena.ucsc.edu/.

Figure 3: Aberrant expression of HMGA2 and KRT80 in ESCC clinical specimens

(Upper) Expression of *HMGA2* in ESCC clinical specimens. Overexpression of HMGA2 was detected in cancer lesions by immunostaining. (Lower) Expression of *KRT80* in ESCC clinical specimens. Overexpression of KRT80 was detected in cancer lesions. In contrast, the expression of KRT80 is hardly observed

in normal epithelium (patient No.18).

Figure 4: Effects of *HMGA2* or KRT80 silencing in ESCC cell lines

(A) *HMGA2* mRNA expression 72 h after transfection with si*HMGA2*-1 and si*HMGA2*-2 in two ESCC cell lines (TE-1 and TE-8). *GAPDH* was used an internal control (*$p < 0.001$). (B) HMGA2 protein expression was evaluated by Western blot analysis 72 h after transfection with si*HMGA2*-1 and si*HMGA2*-2 into ESCC cell lines. GAPDH was used as a loading control. (C) Cell proliferation was identified by XTT assays 72 h after transfection with si*HMGA2*-1 and si*HMGA2*-2 (*$p < 0.001$). (D) Cell migration was measured by wound healing assays (*$p < 0.001$). (E) Cell invasion was determined by Matrigel invasion assays (*$p < 0.001$).
(F) *KRT80* mRNA expression 72 h after transfection with siRNAs, si*KRT80*-1 and si*KRT80*-2 in two ESCC cell lines (TE-1 and TE-8). *GAPDH* was used an internal control (*$p < 0.001$). (G) KRT80 protein expression was evaluated by Western blot analysis. GAPDH was used as a loading control. (H-J) Cell proliferation, migration and invasion assays (*$p < 0.001$).

Supplementary Figure 1: Flowchart of target gene search

The strategy for identification of *miR-143-5p* and miR-143-3p target oncogenes in ESCC cells. We revealed that 6 genes (*HN1*, *HMGA2*, *NETO2*, *STMN1*, *TCF3* and *MET*) were putative targets of *miR-143-5p* regulation, and one gene (*KRT80*) was a putative target of *miR-143-3p* regulation in ESCC cells.

Supplemental Figure 2: Phase micrographs of ESCC cells (TE-1 and TE-8) in migration and invasion assays

Typical phase micrographs of migration and invasion assays by ectopic expression of *miR-143-5p* and *miR-143-3p* in ESCC cell lines (TE-1 and TE-8) are shown.

Supplemental Figure 3A-C: Expression levels of target genes by *miR-143-5p* or *miR-143-3p* regulation in ESCC specimens by TCGA analyses

As for putative targets of *miR-143-5p* or *miR-143-3p*, mRNA expression status of 32 genes (genes not shown in Figure 2) were investigated in ESCC specimens (n = 185) compared to normal specimens (n = 11) (Mann-Whitney test). The expression data were downloaded from http://xena.ucsc.edu/.

Supplementary Figure 4: Direct binding of *miR-143-5p* to *HMGA2* in ESCC cells.

(A,B) Expression levels of *HMGA2*/HMGA2 (mRNA and protein) were significantly reduced by *miR-143-5p* transfection into TE-1 and TE-8 cells (72 h after transfection).

Direct binding of *miR-143-5p* to *HMGA2* in ESCC cells. The TargetScan database showed that 3 putative binding sites of *miR-143-5p* were annotated in the 3′-UTR region of *HMGA2*. (C-E) Dual luciferase reporter assays using vectors encoding the wild-type or deletion-type *miR-143-5p* target site in the *HMGA2* 3'-UTR. Renilla luciferase values were normalized to firefly luciferase values. *$p < 0.001$.

Supplementary Figure 5: Direct binding of *miR-143-3p* to *KRT80* in ESCC cells.

(A,B) Expression levels of *KRT80*/KRT80 (mRNA and protein) were significantly reduced by *miR-143-3p* transfection into TE-1 cells (72 h after transfection).

Direct binding of *miR-143-3p* to *KRT80* in ESCC cells. The TargetScan database showed that one putative binding site of *miR-143-3p* were annotated in the 3′-UTR region of *KRT80*. (C) Dual luciferase reporter assays using vectors encoding the wild-type or deletion-type *miR-143-3p* target site in the *KRT80* 3'-UTR. Renilla luciferase values were normalized to firefly luciferase values. *$p < 0.001$.

Supplementary Figure 6: Expression control of target genes by *miR-143-5p* or *miR-143-3p* regulation in ESCC cell

Expression levels of 6 target genes (*HN1*, *NETO2*, *STMN1*, *TCF3* and *MET*: *miR-143-5p* regulation were evaluated by *miR-143-5p* or *miR-*

143-3p transfected ESCC cells (72 h after miRNAs transfection). *GUSB* was used as an internal control. **p* < 0.001.

Supplementary Figure 7: Aberrant expression of *HMGA2*/HMGA2 in ESCC clinical specimens

(A) Expression of *HMGA2* in ESCC clinical specimens. Overexpression of *HMGA2* was confirmed in ESCC clinical specimens. *GUSB* was used as an internal control. (B) Spearman's rank test showed the negative correlation between *HMGA2* expression and *miR-143-5p* in ESCC clinical specimens.

Supplemental Figure 8: Whole Western blotting images following siRNAs, si*HMGA2*-1 and si*HMGA2*-2, transfection into ESCC cell lines (TE-1 and TE-8)

Supplemental Figure 9: Whole Western blotting images following siRNAs, si*KRT80*-1 and si*KRT80*-2, transfection into ESCC cell lines (TE-1 and TE-8)

Table 1. Downregulated miRNAs in ESCC clinical specimens by RNA sequencing

miRNA	miRbase accesion	Chromosome	FC (log2)	*P* value	FDR
hsa-miR-375	*MIMAT0000728*	chromosome2	-6.6738	1.66E-11	4.29E-08
hsa-miR-1	*MIMAT0000416*	chromosome18 chromosome20	-6.2455	1.97E-08	1.69E-05
hsa-miR-133b	*MIMAT0000770*	chromosome6	-5.9232	3.93E-09	5.07E-06
hsa-miR-206	*MIMAT0000462*	chromosome6	-5.9024	0.000358038	0.035473281
hsa-miR-133a-3p	*MIMAT0000427*	chromosome18 chromosome20	-5.7434	7.10E-08	4.57E-05
hsa-miR-490-3p	*MIMAT0002806*	chromosome7	-5.7181	2.49E-05	0.00458475
hsa-miR-548ba	*MIMAT0031175*	chromosome2	-5.4556	7.10E-05	0.011429197
hsa-miR-208b-3p	*MIMAT0004960*	chromosome14	-5.0191	0.001148595	0.099317996
hsa-miR-135a-5p	*MIMAT0000428*	chromosome3 chromosome12	-4.4576	4.77E-07	0.000204633
hsa-miR-490-5p	*MIMAT0004764*	chromosome7	-4.4345	0.001195209	0.099317996
hsa-miR-6744-5p	*MIMAT0027389*	chromosome11	-3.9395	0.003350167	0.182158033
hsa-miR-133a-5p	*MIMAT0026478*	chromosome18 chromosome20	-3.9132	0.001462949	0.10767302
hsa-miR-6507-5p	*MIMAT0025470*	chromosome10	-3.6750	0.002827128	0.158319149
hsa-miR-488-3p	*MIMAT0004763*	chromosome1	-3.6078	0.0034917	0.182158033
hsa-miR-4705	*MIMAT0019805*	chromosome13	-3.4224	0.001318594	0.099902892
hsa-miR-145-5p	*MIMAT0000437*	chromosome5	-3.2846	1.55E-05	0.003319841
hsa-miR-497-3p	*MIMAT0004768*	chromosome17	-3.2372	0.000277717	0.034066614
hsa-miR-143-3p	*MIMAT0000435*	chromosome5	-3.2017	1.39E-07	7.17E-05
hsa-miR-145-3p	*MIMAT0004601*	chromosome5	-3.1900	1.25E-05	0.003319841
hsa-miR-211-5p	*MIMAT0000268*	chromosome15	-3.0884	0.007022641	0.238030556
hsa-miR-143-5p	*MIMAT0004599*	chromosome5	-2.8946	2.11E-05	0.004174662
hsa-miR-4679	*MIMAT0019763*	chromosome10 chromosome10	-2.8263	0.034292233	0.600930551
hsa-miR-504-5p	*MIMAT0002875*	chromosomeX	-2.7452	0.000357255	0.035473281
hsa-miR-203a	*MIMAT0000264*	chromosome14	-2.4799	0.014915626	0.363623935
hsa-miR-139-3p	*MIMAT0004552*	chromosome11	-2.4441	0.008738731	0.273698299
hsa-miR-30a-5p	*MIMAT0000087*	chromosome6	-2.3938	1.47E-05	0.003319841
hsa-miR-139-5p	*MIMAT0000250*	chromosome11	-2.2908	0.000805511	0.074107036
hsa-miR-30a-3p	*MIMAT0000088*	chromosome6	-2.2084	0.000109003	0.016517129
hsa-miR-3617-5p	*MIMAT0017997*	chromosome20	-2.2043	0.043564984	0.685371179
hsa-miR-422a	*MIMAT0001339*	chromosome15	-2.1396	0.041953793	0.674849786
hsa-miR-3195	*MIMAT0015079*	chromosome20	-2.0025	0.011922647	0.329980536
hsa-miR-551b-3p	*MIMAT0003233*	chromosome3	-1.8995	0.025787082	0.492055735
hsa-miR-1260a	*MIMAT0005911*	chromosome14	-1.8212	0.032579702	0.582814665
hsa-miR-887-3p	*MIMAT0004951*	chromosome5	-1.7768	0.007253881	0.239564079
hsa-miR-30c-2-3p	*MIMAT0004550*	chromosome6	-1.7435	0.005478903	0.220525842
hsa-miR-1260b	*MIMAT0015041*	chromosome11	-1.6727	0.026523856	0.495111986
hsa-miR-328-3p	*MIMAT0000752*	chromosome16	-1.6194	0.008453039	0.268827523
hsa-miR-28-5p	*MIMAT0000085*	chromosome3	-1.5182	0.007726705	0.248799893
hsa-miR-29c-5p	*MIMAT0004673*	chromosome1	-1.4931	0.01465692	0.363623935
hsa-miR-378a-5p	*MIMAT0000731*	chromosome5	-1.4914	0.021683269	0.450452421
hsa-miR-378d	*MIMAT0018926*	chromosome8 chromosome4	-1.4886	0.017547559	0.392351221
hsa-miR-10b-5p	*MIMAT0000254*	chromosome2	-1.4623	0.011645257	0.32606719
hsa-miR-195-5p	*MIMAT0000461*	chromosome17	-1.3952	0.042178112	0.674849786
hsa-miR-378a-3p	*MIMAT0000732*	chromosome5	-1.3805	0.01407219	0.363623935
hsa-miR-30c-5p	*MIMAT0000244*	chromosome6 chromosome1	-1.2456	0.02035509	0.433344733
hsa-miR-28-3p	*MIMAT0004502*	chromosome3	-1.2086	0.02516218	0.490667928
hsa-miR-664a-3p	*MIMAT0005949*	chromosome1	-1.2070	0.039011206	0.639841129

Table 2A. Candidate of *miR-143-5p* targets in ESCC cells

Entrez Gene ID	Gene Symbol	Gene name	TE-1 *miR-143-5p* transfectant FC (log2)	TE-8 *miR-143-5p* transfectant FC (log2)	Mean FC (log2)	Total binding sites
51155	*HN1*	hematological and neurological expressed 1	-2.59	-1.88	-2.24	1
8091	*HMGA2*	high mobility group AT-hook 2	-2.25	-2.02	-2.13	3
26035	*GLCE*	glucuronic acid epimerase	-2.05	-1.73	-1.89	3
100532736	*HAS3*	hyaluronan synthase 3	-1.63	-2.05	-1.84	2
1809	*MINOS1-NBL1*	MINOS1-NBL1 readthrough	-1.96	-1.57	-1.76	1
5515	*DPYSL3*	dihydropyrimidinase-like 3	-1.92	-1.50	-1.71	2
3038	*PPP2CA*	protein phosphatase 2, catalytic subunit, alpha isozyme	-1.88	-1.22	-1.55	1
57706	*DENND1A*	DENN/MADD domain containing 1A	-1.57	-1.50	-1.54	1
285381	*CDK14*	cyclin-dependent kinase 14	-1.47	-1.58	-1.53	2
5218	*NETO2*	neuropilin (NRP) and tolloid (TLL)-like 2	-1.45	-1.55	-1.50	1
3925	*CAV1*	caveolin 1, caveolae protein, 22kDa	-1.18	-1.79	-1.49	1
285362	*DPH3*	diphthamide biosynthesis 3	-1.53	-1.42	-1.48	2
81831	*ESYT1*	extended synaptotagmin-like protein 1	-1.34	-1.54	-1.44	2
84317	*CCDC115*	coiled-coil domain containing 115	-1.41	-1.40	-1.41	1
84317	*FMR1*	fragile X mental retardation 1	-1.32	-1.44	-1.38	1
10966	*MAK16*	MAK16 homolog (S. cerevisiae)	-1.39	-1.33	-1.36	1
84317	*RAB40B*	RAB40B, member RAS oncogene family	-1.37	-1.19	-1.28	1
23344	*DIRC2*	disrupted in renal carcinoma 2	-1.36	-1.19	-1.27	2
2332	*STMN1*	stathmin 1	-1.46	-1.08	-1.27	1
55666	*SUMF1*	sulfatase modifying factor 1	-1.46	-1.05	-1.25	1
25960	*GPR124*	G protein-coupled receptor 124	-1.21	-1.25	-1.23	1
23241	*CARD10*	caspase recruitment domain family, member 10	-1.11	-1.28	-1.19	1
55643	*NPLOC4*	nuclear protein localization 4 homolog (S. cerevisiae)	-1.29	-1.08	-1.19	3
8111	*MTFR1*	mitochondrial fission regulator 1	-1.14	-1.19	-1.16	1
9650	*PACS2*	phosphofurin acidic cluster sorting protein 2	-1.16	-1.14	-1.15	1
6929	*BTBD2*	BTB (POZ) domain containing 2	-1.16	-1.13	-1.15	1
57505	*AARS2*	alanyl-tRNA synthetase 2, mitochondrial	-1.11	-1.14	-1.13	3
29775	*GPR68*	G protein-coupled receptor 68	-1.14	-1.10	-1.12	1
4233	*TCF3*	transcription factor 3	-1.11	-1.08	-1.10	2
2332	*MET*	met proto-oncogene	-1.09	-1.06	-1.08	1
113000	*RPUSD1*	RNA pseudouridylate synthase domain containing 1	-1.01	-1.01	-1.01	1

Table 2B. Candidate of *miR-143-3p* targets in ESCC cells

Entrez Gene ID	Gene Symbol	Gene name	TE-1 *miR-143-3p* transfectant FC (log2)	TE-8 *miR-143-3p* transfectant FC (log2)	Mean FC (log2)	Total binding sites
3038	*HAS3*	hyaluronan synthase 3	-2.21	-1.71	-1.96	2
144501	*KRT80*	keratin 80, type II	-1.69	-2.13	-1.91	1
5349	*FXYD3*	FXYD domain containing ion transport regulator 3	-2.16	-1.08	-1.62	1
5916	*RARG*	retinoic acid receptor, gamma	-1.44	-1.37	-1.41	1
7170	*TPM3*	tropomyosin 3	-1.52	-1.04	-1.28	3
2581	*GALC*	galactosylceramidase	-1.34	-1.14	-1.24	2
55616	*ASAP3*	ArfGAP with SH3 domain, ankyrin repeat and PH domain 3	-1.39	-1.03	-1.21	3
28996	*HIPK2*	homeodomain interacting protein kinase 2	-1.21	-1.16	-1.18	10
51280	*GOLM1*	golgi membrane protein 1	-1.18	-1.05	-1.11	3

Figure 1

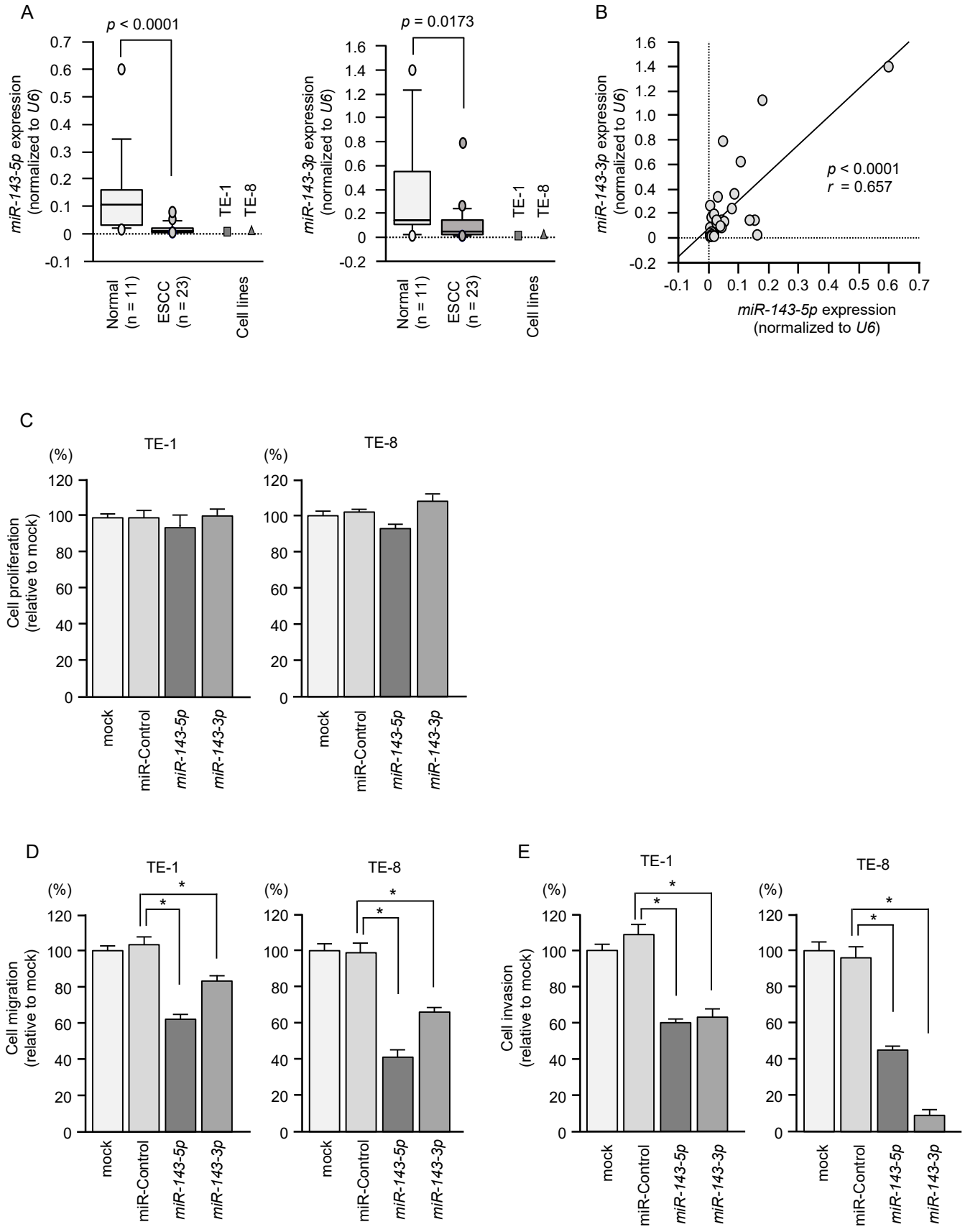
A
p < 0.0001
miR-143-5p expression (normalized to U6)
Normal (n = 11)
ESCC (n = 23)
Cell lines
TE-1
TE-8
p = 0.0173
miR-143-3p expression (normalized to U6)
B
p < 0.0001
r = 0.657
miR-143-5p expression (normalized to U6)
C
TE-1
TE-8
(%)
Cell proliferation (relative to mock)
mock
miR-Control
miR-143-5p
miR-143-3p
D
Cell migration (relative to mock)
E
Cell invasion (relative to mock)

Figure 2

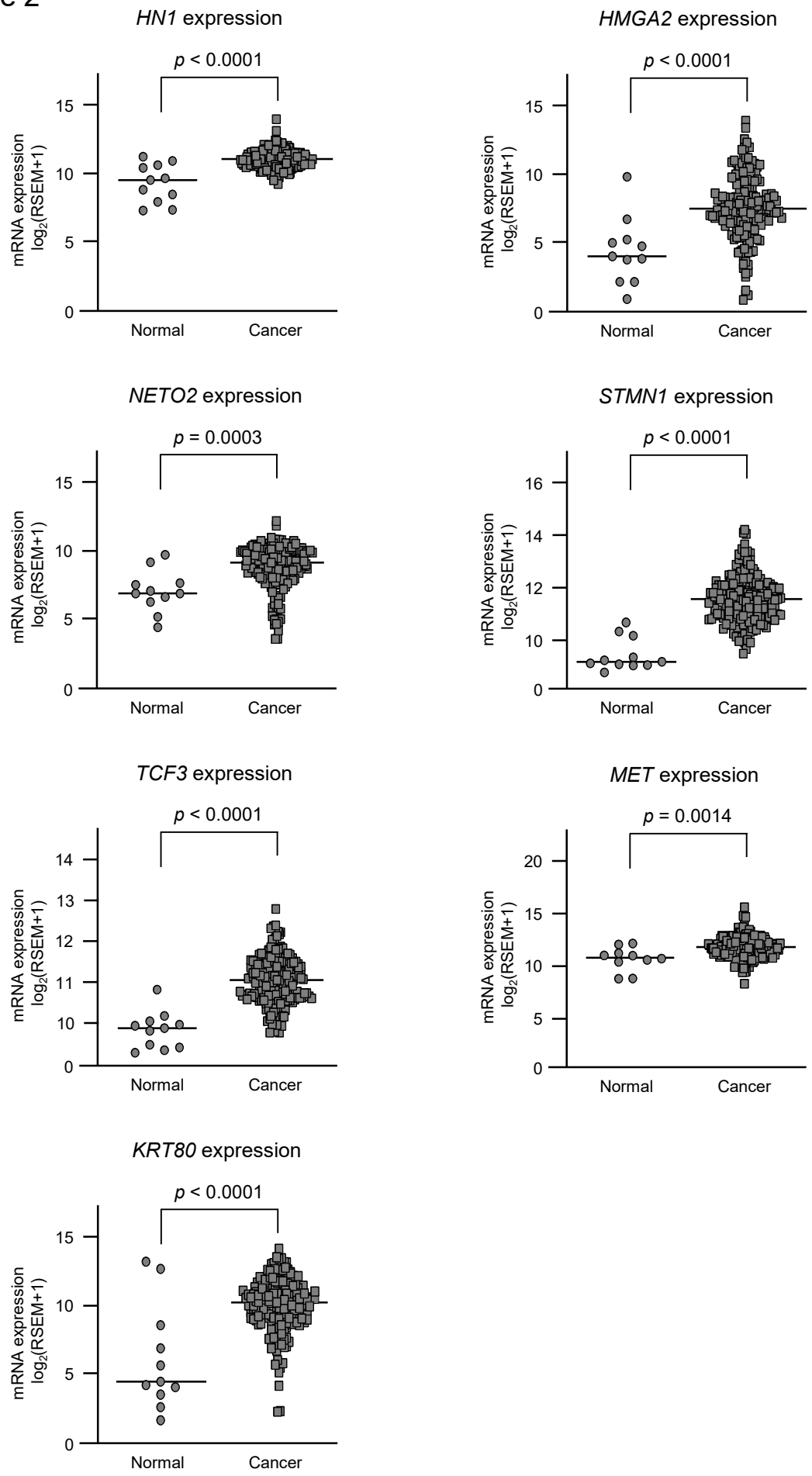
HN1 expression
p < 0.0001
HMGA2 expression
p < 0.0001
NETO2 expression
p = 0.0003
STMN1 expression
p < 0.0001
TCF3 expression
p < 0.0001
MET expression
p = 0.0014
KRT80 expression
p < 0.0001
mRNA expression log2(RSEM+1)
Normal
Cancer

Figure 3

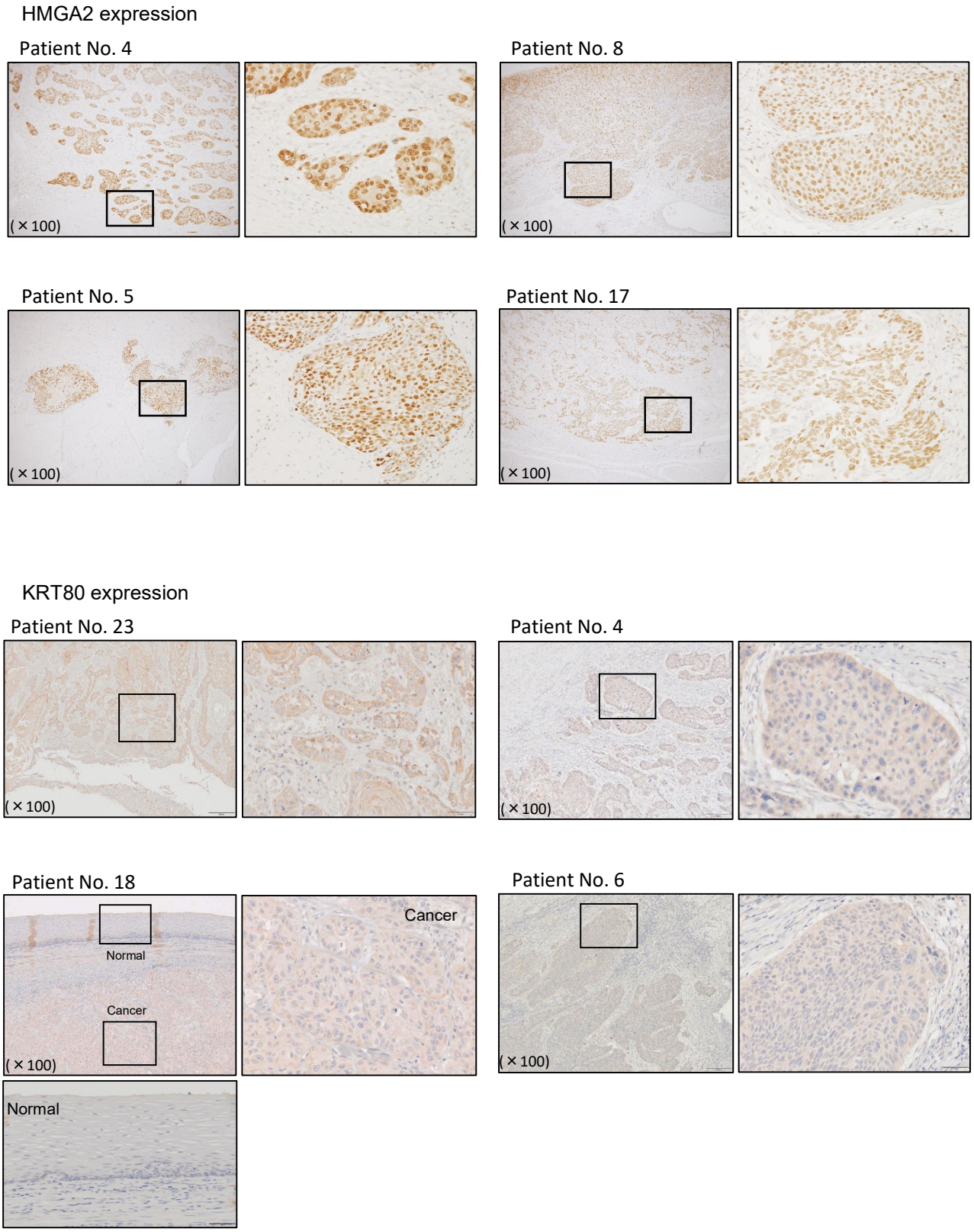
HMGA2 expression
Patient No. 4
(×100)
Patient No. 8
(×100)
Patient No. 5
(×100)
Patient No. 17
(×100)
KRT80 expression
Patient No. 23
(×100)
Patient No. 4
(×100)
Patient No. 18
Normal
Cancer
(×100)
Cancer
Normal
Patient No. 6
(×100)

Figure 4

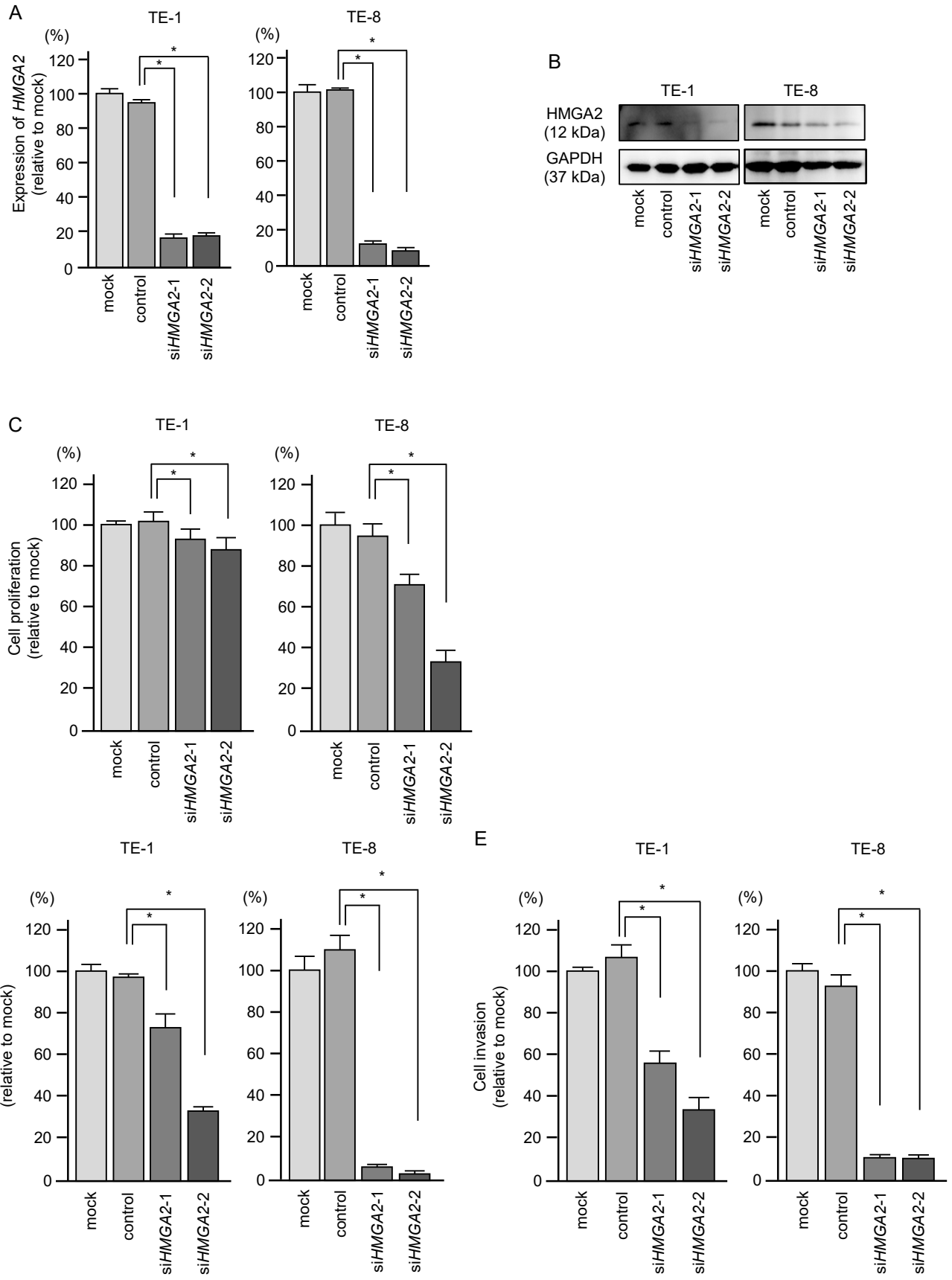
A
TE-1
TE-8
(%)
Expression of HMGA2 (relative to mock)
120
100
80
60
40
20
0
*
mock
control
siHMGA2-1
siHMGA2-2
B
TE-1
TE-8
HMGA2 (12 kDa)
GAPDH (37 kDa)
mock
control
siHMGA2-1
siHMGA2-2
C
TE-1
TE-8
(%)
Cell proliferation (relative to mock)
D
TE-1
TE-8
(%)
Cell migration (relative to mock)
E
TE-1
TE-8
(%)
Cell invasion (relative to mock)

Figure 4

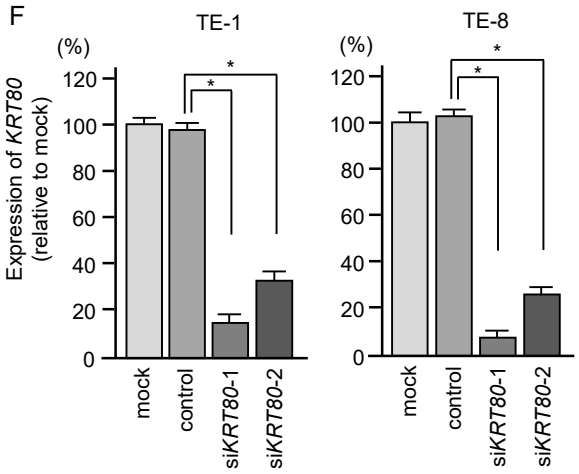
F
TE-1
TE-8
(%)
Expression of KRT80
(relative to mock)
120
100
80
60
40
20
0
*
mock
control
siKRT80-1
siKRT80-2

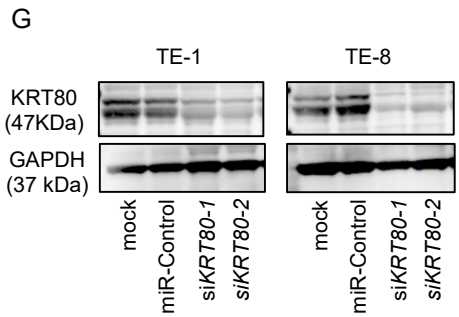
G
TE-1
TE-8
KRT80
(47KDa)
GAPDH
(37 kDa)
mock
miR-Control
siKRT80-1
siKRT80-2

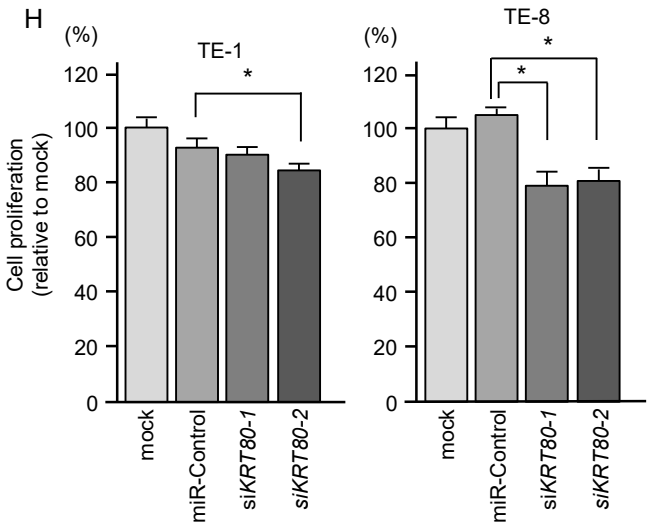
H
TE-1
TE-8
(%)
Cell proliferation
(relative to mock)
120
100
80
60
40
20
0
*
mock
miR-Control
siKRT80-1
siKRT80-2

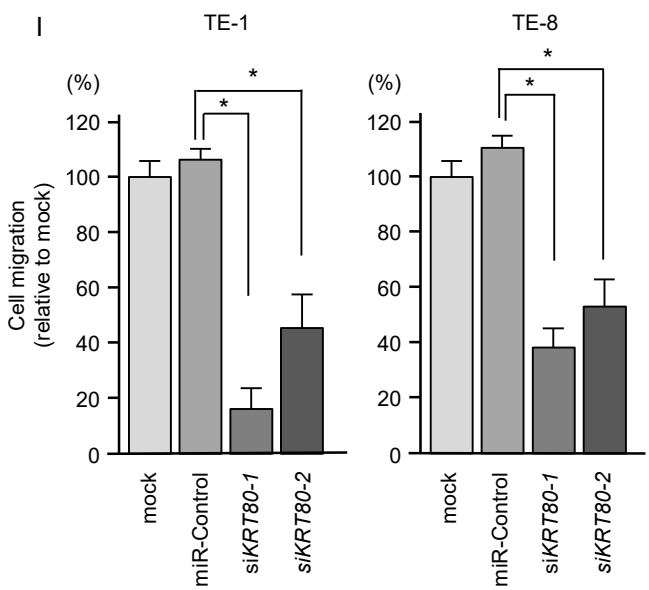
I
TE-1
TE-8
(%)
Cell migration
(relative to mock)
120
100
80
60
40
20
0
*
mock
miR-Control
siKRT80-1
siKRT80-2

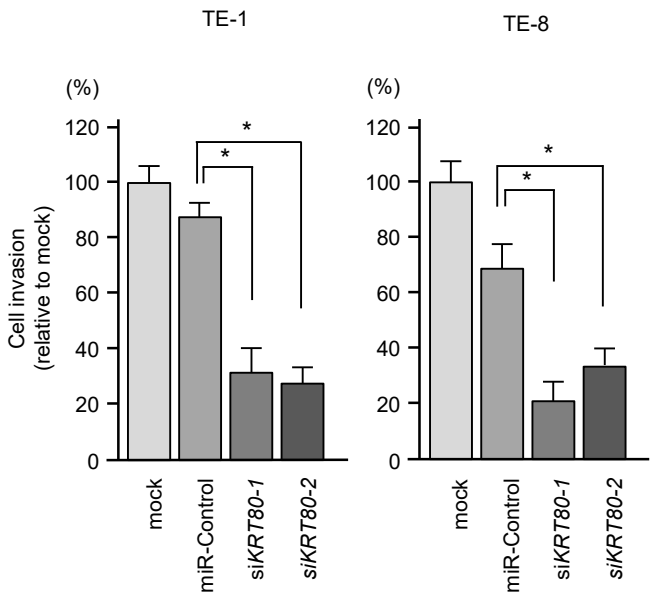
TE-1
TE-8
(%)
Cell invasion
(relative to mock)
120
100
80
60
40
20
0
*
mock
miR-Control
siKRT80-1
siKRT80-2

Supplementary Table 1. Clinicopathological features of patients with ESCC (RNA-sequencing)

No.	Specimen	Age (years)	Sex	Differentiation	T	N	M	Stage	ly	v	Recurrence
1	ESCC	56	Male	moderate	2	0	0	IIA	0	1	-
2		79	Male	moderate	2	1	0	IIB	1	1	+
3		78	Male	well	3	0	0	IIA	1	2	-
4		71	Male	moderate	3	0	0	IIA	1	2	-
5	Normal	56	Male								
6		79	Male								
7		78	Male								
8		71	Male								

ly, lymphatic invasion; M, metastasis; N, nodes; T, tumor; v, venous invasion.

Supplementary Table 1. Clinicopathological features of patients with ESCC (validation)

No.	Age (years)	Sex	Differentiation	T	N	M	Stage	ly	v	Recurrence
1	68	Male	poor	1b	2	0	IIIA	1	3	+
2	72	Male	moderate	1b	0	0	IA	0	1	-
3	69	Male	moderate	1b	0	0	IA	0	0	-
4	66	Male	moderate	3	0	0	IIA	1	1	-
5	74	Male	moderate	2	2	0	IIIA	3	1	+
6	56	Male	moderate	2	0	0	IB	0	1	-
7	79	Male	moderate	2	1	0	IIB	1	1	-
8	68	Male	moderate	1b	2	0	IIIA	1	1	-
9	52	Male	poor	1b	0	0	IA	1	1	+
10	67	Male	well	3	2	0	IIIB	2	2	+
11	57	Male	poor	3	3	0	IIIC	1	1	+
12	70	Male	moderate	3	0	0	IIA	1	1	+
13	66	Male	moderate	3	0	0	IIA	1	1	-
14	63	Male	well	3	3	0	IIIC	2	1	+
15	55	Male	moderate	3	2	0	IIIB	1	1	+
16	60	Male	well	1b	1	0	IIB	1	1	-
17	77	Male	poor	1b	1	0	IIB	1	1	-
18	71	Male	moderate	3	0	0	IIA	1	2	-
19	75	Male	moderate	3	2	0	IIIB	1	1	+
20	60	Male	moderate	2	1	0	IIB	1	2	+
21	62	Male	moderate	1a	1	0	IIB	0	0	+
22	69	Male	moderate	1b	0	0	IA	1	0	-
23	84	Male	well	2	1	0	IIB	1	1	-

ly, lymphatic invasion; M, metastasis; N, nodes; T, tumor; v, venous invasion.

Noncancerous esophageal tissues were collected by patients with ESCC

No.	Age (years)	Sex
1	66	Male
2	52	Male
3	78	Male
4	75	Male
5	60	Male
6	71	Male
7	64	Male
8	79	Female
9	81	Male
10	69	Male
11	84	Male

Supplementary Table 2. Reagents used in this study

TaqMan primers and probes	Assay ID	Company
hsa-miR-143-5p	002146	Applied Biosystems, Waltham, MA, USA
hsa-miR-143-3p	002249	Applied Biosystems, Waltham, MA, USA
hsa-miR-21	000397	Applied Biosystems, Waltham, MA, USA
U6	001973	Applied Biosystems, Waltham, MA, USA
HMGA2	Hs04397751_m1	Applied Biosystems, Waltham, MA, USA
MET	Hs01565584_m1	Applied Biosystems, Waltham, MA, USA
CDK14	Hs00202633_m1	Applied Biosystems, Waltham, MA, USA
DPYSL3	Hs00181665_m1	Applied Biosystems, Waltham, MA, USA
NETO2	Hs00983152_m1	Applied Biosystems, Waltham, MA, USA
TCF3	Hs01012685_m1	Applied Biosystems, Waltham, MA, USA
STMN1	Hs01027515_gH	Applied Biosystems, Waltham, MA, USA
KRT80	Hs01372365_m1	Applied Biosystems, Waltham, MA, USA
GUSB	Hs99999908_m1	Applied Biosystems, Waltham, MA, USA

pre-miR miRNA presursors	Assay ID	Concentration	
miR-143-5p	PM12540	10 nM	Applied Biosystems, Waltham, MA, USA
miR-143-3p	PM 10883	10 nM	Applied Biosystems, Waltham, MA, USA
negative control miRNA #1	AM17010	10 nM	Applied Biosystems, Waltham, MA, USA

Stealth RNAi siRNA	Assay ID	Concentration	
HMGA2	HSS188538 HSS188539	10 nM	Applied Biosystems, Waltham, MA, USA
KRT80	HSS175355 HSS175356	10 nM	Applied Biosystems, Waltham, MA, USA

antibody	catalog number	dilution	
Anti-HMGA2	ab97276	WB 1:1000	Abcam, Cambridge, UK
	ab52039	IHC 1:400	
Anti-KRT80	16835-1-AP	WB 1:1500 IHC 1:400	Proteintech Group, Rosemont, USA
GAPDH	SAF6698	WB 1:1500	Wako, Osaka, Japan

Supplementary Table 3. Annotation of reads alignment to small RNAs

ESCC samples	ESCC1		ESCC2		ESCC3		ESCC4	
	Count	(%)	Count	(%)	Count	(%)	Count	(%)
Total	33,142,055	100	33,253,231	100	28,559,303	100	31,587,854	100
exon	495,864	1.50	935,524	2.81	420,483	1.47	545,462	1.73
exon_antisense	23	0.00	39	0.00	5	0.00	0	0.00
miRNA	10,399,997	31.38	17,132,134	51.52	14,098,700	49.37	6,314,266	19.99
rRNA	128,215	0.39	344,260	1.04	269,403	0.94	236,384	0.75
tRNA	4,337,724	13.09	1,893,147	5.69	2,164,263	7.58	7,289,871	23.08
snRNA	15,673	0.05	36,771	0.11	20,449	0.07	20,792	0.07
snoRNA	370,233	1.12	313,485	0.94	269,900	0.95	249,601	0.79
lcnRNA	230	0.00	453	0.00	107	0.00	503	0.00
ribozyme	7,384	0.02	5,283	0.02	7,545	0.03	6,486	0.02
sRNA	122	0.00	170	0.00	95	0.00	82	0.00
Unannotated	4,170,646	12.58	4,600,385	13.83	1,498,386	5.25	2,771,394	8.77
Unmapped	13,215,944	39.88	7,991,580	24.03	9,809,967	34.35	14,153,013	44.81

Normal samples	N1		N2		N3		N4	
	Count	(%)	Count	(%)	Count	(%)	Count	(%)
Total	27,864,484	100	30,271,013	100	30,364,458	100	31,046,926	100
exon	263,239	0.94	266,233	0.88	102,996	0.34	236,099	0.76
exon_antisense	13	0.00	4	0.00	5	0.00	2	0.00
miRNA	16,409,173	58.89	26,123,671	86.30	13,225,458	43.56	17,334,705	55.83
rRNA	136,391	0.49	49,513	0.16	69,814	0.23	213,171	0.69
tRNA	1,795,091	6.44	452,982	1.50	4,149,131	13.66	2,864,950	9.23
snRNA	4,756	0.02	3,167	0.01	3,326	0.01	7,578	0.02
snoRNA	825,532	2.96	112,429	0.37	97,485	0.32	339,186	1.09
lcnRNA	102	0.00	86	0.00	54	0.00	123	0.00
ribozyme	8,600	0.03	1,310	0.00	2,351	0.01	2,911	0.01
sRNA	66	0.00	28	0.00	82	0.00	32	0.00
Unannotated	1,016,415	3.65	651,778	2.15	492,214	1.62	1,281,797	4.13
Unmapped	7,765,106	27.87	2,609,812	8.62	12,221,542	40.25	8,766,372	28.24

Supplementary Table 4. Downregulated genes in *siHMGA2* transfected TE-8 cells

Entrez Gene ID	Gene Symbol	Gene name	TE-8 *siHMGA2* transfectant FC (log 2)
83879	*CDCA7*	cell division cycle associated 7	-4.83
2023	*ENO1*	enolase 1, (alpha)	-4.02
2305	*FOXM1*	forkhead box M1	-3.99
11013	*TMSB15A*	thymosin beta 15a	-3.97
3024	*HIST1H1A*	histone cluster 1, H1a	-3.86
3397	*ID1*	inhibitor of DNA binding 1, dominant negative helix-loop-helix protein	-3.74
10874	*NMU*	neuromedin U	-3.66
161291	*TMEM30B*	transmembrane protein 30B	-3.64
3866	*KRT15*	keratin 15, type I	-3.63
51176	*LEF1*	lymphoid enhancer-binding factor 1	-3.61
26022	*TMEM98*	transmembrane protein 98	-3.59
128178	*EDARADD*	EDAR-associated death domain	-3.53
203328	*SUSD3*	sushi domain containing 3	-3.52
27074	*LAMP3*	lysosomal-associated membrane protein 3	-3.48
4001	*LMNB1*	lamin B1	-3.48
3161	*HMMR*	hyaluronan-mediated motility receptor (RHAMM)	-3.45
4288	*MKI67*	marker of proliferation Ki-67	-3.43
3009	*HIST1H1B*	histone cluster 1, H1b	-3.41
2877	*GPX2*	glutathione peroxidase 2 (gastrointestinal)	-3.40
999	*CDH1*	cadherin 1, type 1, E-cadherin (epithelial)	-3.39
3832	*KIF11*	kinesin family member 11	-3.38
84823	*LMNB2*	lamin B2	-3.33
157570	*ESCO2*	establishment of sister chromatid cohesion N-acetyltransferase 2	-3.32
580	*BARD1*	BRCA1 associated RING domain 1	-3.29
1870	*E2F2*	E2F transcription factor 2	-3.28
81610	*FAM83D*	family with sequence similarity 83, member D	-3.25
3148	*HMGB2*	high mobility group box 2	-3.24
3800	*KIF5C*	kinesin family member 5C	-3.23
3667	*IRS1*	insulin receptor substrate 1	-3.20
51203	*NUSAP1*	nucleolar and spindle associated protein 1	-3.20
11113	*CIT*	citron rho-interacting serine/threonine kinase	-3.19
10112	KIF20A	kinesin family member 20A	-3.14
8329	HIST1H2AI	histone cluster 1, H2ai	-3.13
133418	EMB	embigin	-3.13
29128	UHRF1	ubiquitin-like with PHD and ring finger domains 1	-3.12
57582	KCNT1	potassium channel, sodium activated subfamily T, member 1	-3.11
2281	FKBP1B	FK506 binding protein 1B, 12.6 kDa	-3.11
29089	UBE2T	ubiquitin-conjugating enzyme E2T	-3.11
57452	GALNT16	polypeptide N-acetylgalactosaminyltransferase 16	-3.11
3852	KRT5	keratin 5, type II	-3.10
56992	KIF15	kinesin family member 15	-3.08
55222	LRRC20	leucine rich repeat containing 20	-3.07
333932	HIST2H3A	histone cluster 2, H3a	-3.04
1058	CENPA	centromere protein A	-3.04
3553	IL1B	interleukin 1, beta	-3.03
9355	LHX2	LIM homeobox 2	-3.02
8358	HIST1H3B	histone cluster 1, H3b	-2.99
100506211	MIR210HG	MIR210 host gene (non-protein coding)	-2.98
54820	NDE1	nudE neurodevelopment protein 1	-2.98
4907	NT5E	5'-nucleotidase, ecto (CD73)	-2.98
9534	ZNF254	zinc finger protein 254	-2.93
10202	DHRS2	dehydrogenase/reductase (SDR family) member 2	-2.92
7298	TYMS	thymidylate synthetase	-2.91
259266	ASPM	asp (abnormal spindle) homolog, microcephaly associated (Drosophila)	-2.91

55698	RADIL	Ras association and DIL domains	-2.91
3898	LAD1	ladinin 1	-2.89
5427	POLE2	polymerase (DNA directed), epsilon 2, accessory subunit	-2.88
397	ARHGDIB	Rho GDP dissociation inhibitor (GDI) beta	-2.85
51512	GTSE1	G-2 and S-phase expressed 1	-2.84
83999	KREMEN1	kringle containing transmembrane protein 1	-2.84
83543	AIF1L	allograft inflammatory factor 1-like	-2.83
81543	LRRC3	leucine rich repeat containing 3	-2.83
2300	FOXL1	forkhead box L1	-2.81
145773	FAM81A	family with sequence similarity 81, member A	-2.80
1958	EGR1	early growth response 1	-2.80
2237	FEN1	flap structure-specific endonuclease 1	-2.79
6941	TCF19	transcription factor 19	-2.78
3833	KIFC1	kinesin family member C1	-2.78
1719	DHFR	dihydrofolate reductase	-2.78
4312	MMP1	matrix metallopeptidase 1 (interstitial collagenase)	-2.78
4232	MEST	mesoderm specific transcript	-2.76
8969	HIST1H2AG	histone cluster 1, H2ag	-2.76
51514	DTL	denticleless E3 ubiquitin protein ligase homolog (Drosophila)	-2.75
51659	GINS2	GINS complex subunit 2 (Psf2 homolog)	-2.75
3007	HIST1H1D	histone cluster 1, H1d	-2.75
9221	NOLC1	nucleolar and coiled-body phosphoprotein 1	-2.75
3920	LAMP2	lysosomal-associated membrane protein 2	-2.73
728833	FAM72D	family with sequence similarity 72, member D	-2.73
286887	KRT6C	keratin 6C, type II	-2.73
9134	CCNE2	cyclin E2	-2.72
81563	C1orf21	chromosome 1 open reading frame 21	-2.72
100037417	DDTL	D-dopachrome tautomerase-like	-2.72
79109	MAPKAP1	mitogen-activated protein kinase associated protein 1	-2.71
4998	ORC1	origin recognition complex, subunit 1	-2.71
9133	CCNB2	cyclin B2	-2.70
5230	PGK1	phosphoglycerate kinase 1	-2.70
55165	CEP55	centrosomal protein 55kDa	-2.69
3757	KCNH2	potassium channel, voltage gated eag related subfamily H, member 2	-2.69
6929	TCF3	transcription factor 3	-2.69
9768	KIAA0101	KIAA0101	-2.68
3092	HIP1	huntingtin interacting protein 1	-2.66
4900	NRGN	neurogranin (protein kinase C substrate, RC3)	-2.66
84969	TOX2	TOX high mobility group box family member 2	-2.66
201725	C4orf46	chromosome 4 open reading frame 46	-2.65
3184	HNRNPD	heterogeneous nuclear ribonucleoprotein D (AU-rich element RNA binding	-2.65
283131	NEAT1	nuclear paraspeckle assembly transcript 1 (non-protein coding)	-2.65
84951	TNS4	tensin 4	-2.65
55872	PBK	PDZ binding kinase	-2.65
28988	DBNL	drebrin-like	-2.64
221150	SKA3	spindle and kinetochore associated complex subunit 3	-2.62
7153	TOP2A	topoisomerase (DNA) II alpha 170kDa	-2.62
6470	SHMT1	serine hydroxymethyltransferase 1 (soluble)	-2.61
79875	THSD4	thrombospondin, type I, domain containing 4	-2.61
11130	ZWINT	ZW10 interacting kinetochore protein	-2.60
6241	RRM2	ribonucleotide reductase M2	-2.60
55344	PLCXD1	phosphatidylinositol-specific phospholipase C, X domain containing 1	-2.59
124222	PAQR4	progestin and adipoQ receptor family member IV	-2.59
196513	DCP1B	decapping mRNA 1B	-2.57
3853	KRT6A	keratin 6A, type II	-2.56
10024	TROAP	trophinin associated protein	-2.56
647087	C7orf73	chromosome 7 open reading frame 73	-2.56
701	BUB1B	BUB1 mitotic checkpoint serine/threonine kinase B	-2.55
8331	HIST1H2AJ	histone cluster 1, H2aj	-2.55

7089	TLE2	transducin-like enhancer of split 2	-2.55
50964	SOST	sclerostin	-2.53
10360	NPM3	nucleophosmin/nucleoplasmin 3	-2.52
100507050	TPBGL	trophoblast glycoprotein-like	-2.52
8357	HIST1H3H	histone cluster 1, H3h	-2.52
201799	TMEM154	transmembrane protein 154	-2.52
83742	MARVELD1	MARVEL domain containing 1	-2.51
169611	OLFML2A	olfactomedin-like 2A	-2.51
57333	RCN3	reticulocalbin 3, EF-hand calcium binding domain	-2.51
655	BMP7	bone morphogenetic protein 7	-2.51
374	AREG	amphiregulin	-2.51
5359	PLSCR1	phospholipid scramblase 1	-2.50
55055	ZWILCH	zwilch kinetochore protein	-2.50
827	CAPN6	calpain 6	-2.50
6503	SLA	Src-like-adaptor	-2.49
8438	RAD54L	RAD54-like (S. cerevisiae)	-2.49
92196	DAPL1	death associated protein-like 1	-2.49
8368	HIST1H4L	histone cluster 1, H4l	-2.48
10435	CDC42EP2	CDC42 effector protein (Rho GTPase binding) 2	-2.48
56896	DPYSL5	dihydropyrimidinase-like 5	-2.48
79827	CLMP	CXADR-like membrane protein	-2.47
5321	PLA2G4A	phospholipase A2, group IVA (cytosolic, calcium-dependent)	-2.47
171568	POLR3H	polymerase (RNA) III (DNA directed) polypeptide H (22.9kD)	-2.47
11202	KLK8	kallikrein-related peptidase 8	-2.47
84695	LOXL3	lysyl oxidase-like 3	-2.46
3613	IMPA2	inositol(myo)-1(or 4)-monophosphatase 2	-2.46
83990	BRIP1	BRCA1 interacting protein C-terminal helicase 1	-2.46
10376	TUBA1B	tubulin, alpha 1b	-2.45
8534	CHST1	carbohydrate (keratan sulfate Gal-6) sulfotransferase 1	-2.45
8738	CRADD	CASP2 and RIPK1 domain containing adaptor with death domain	-2.45
90381	TICRR	TOPBP1-interacting checkpoint and replication regulator	-2.44
79866	BORA	bora, aurora kinase A activator	-2.44
81930	KIF18A	kinesin family member 18A	-2.43
2175	FANCA	Fanconi anemia, complementation group A	-2.42
3005	H1F0	H1 histone family, member 0	-2.42
79102	RNF26	ring finger protein 26	-2.42
4176	MCM7	minichromosome maintenance complex component 7	-2.42
54821	ERCC6L	excision repair cross-complementation group 6-like	-2.42
10921	RNPS1	RNA binding protein S1, serine-rich domain	-2.41
8971	H1FX	H1 histone family, member X	-2.41
8448	DOC2A	double C2-like domains, alpha	-2.41
8364	HIST1H4C	histone cluster 1, H4c	-2.41
8968	HIST1H3F	histone cluster 1, H3f	-2.41
29899	GPSM2	G-protein signaling modulator 2	-2.41
79019	CENPM	centromere protein M	-2.40
55536	CDCA7L	cell division cycle associated 7-like	-2.40
55269	PSPC1	paraspeckle component 1	-2.39
7145	TNS1	tensin 1	-2.39
91860	CALML4	calmodulin-like 4	-2.39
2171	FABP5	fatty acid binding protein 5 (psoriasis-associated)	-2.38
90525	SHF	Src homology 2 domain containing F	-2.38
8091	HMGA2	high mobility group AT-hook 2	-2.38
55388	MCM10	minichromosome maintenance complex component 10	-2.37
147841	SPC24	SPC24, NDC80 kinetochore complex component	-2.36
5557	PRIM1	primase, DNA, polypeptide 1 (49kDa)	-2.36
2069	EREG	epiregulin	-2.35
699	BUB1	BUB1 mitotic checkpoint serine/threonine kinase	-2.35
8636	SSNA1	Sjogren syndrome nuclear autoantigen 1	-2.35
574036	SERTAD4-AS1	SERTAD4 antisense RNA 1	-2.35

55355	HJURP	Holliday junction recognition protein	-2.35
124590	USH1G	Usher syndrome 1G (autosomal recessive)	-2.35
89944	GLB1L2	galactosidase, beta 1-like 2	-2.35
3070	HELLS	helicase, lymphoid-specific	-2.35
6542	SLC7A2	solute carrier family 7 (cationic amino acid transporter, y+ system), membe	-2.35
100506411	LOC100506411	uncharacterized LOC100506411	-2.34
4610	MYCL	v-myc avian myelocytomatosis viral oncogene lung carcinoma derived hon	-2.34
1718	DHCR24	24-dehydrocholesterol reductase	-2.34
2013	EMP2	epithelial membrane protein 2	-2.34
30818	KCNIP3	Kv channel interacting protein 3, calsenilin	-2.33
121504	HIST4H4	histone cluster 4, H4	-2.33
8801	SUCLG2	succinate-CoA ligase, GDP-forming, beta subunit	-2.33
647024	C6orf132	chromosome 6 open reading frame 132	-2.33
3916	LAMP1	lysosomal-associated membrane protein 1	-2.33
8519	IFITM1	interferon induced transmembrane protein 1	-2.32
90355	C5orf30	chromosome 5 open reading frame 30	-2.32

Supplemental Figure 1

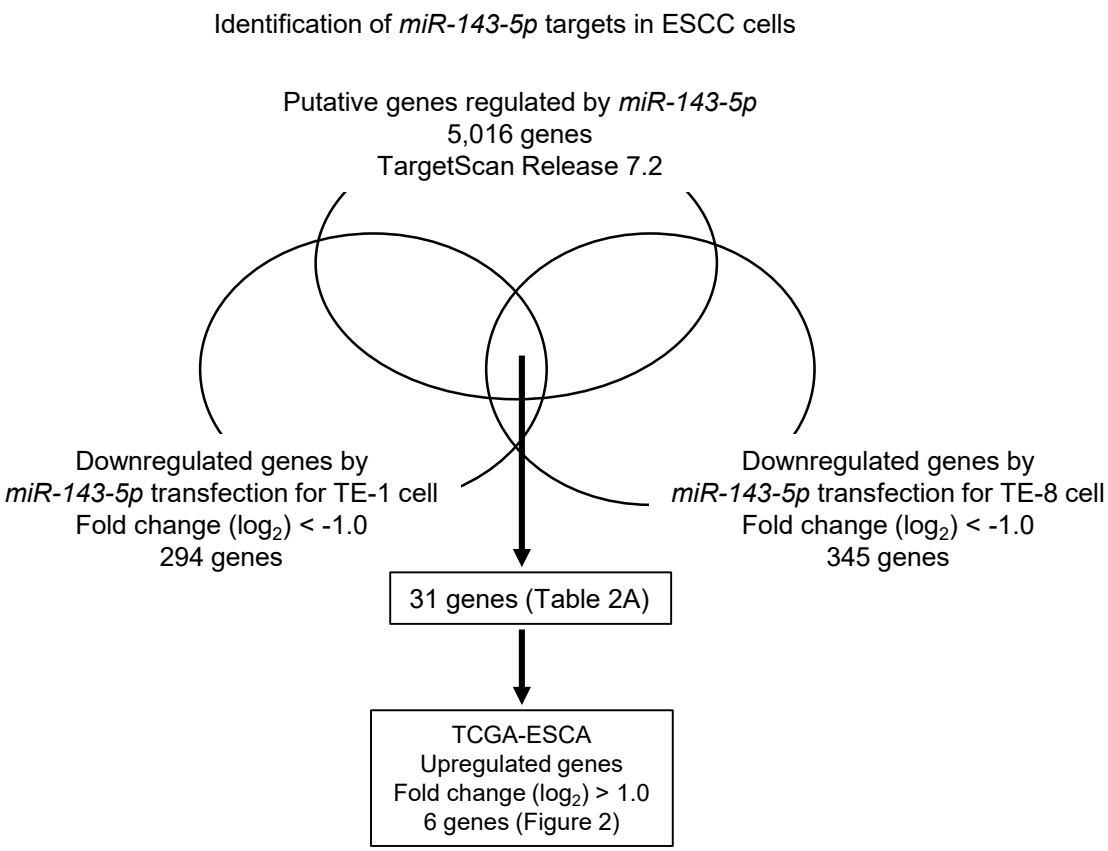

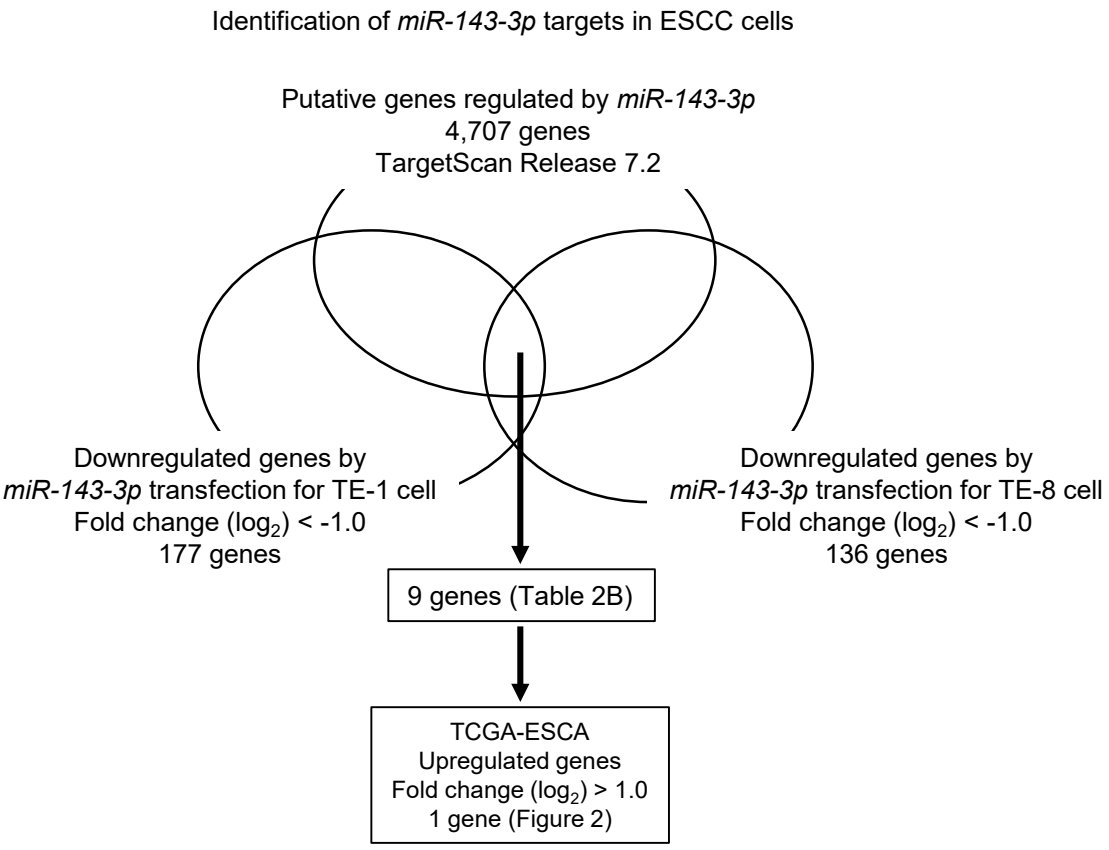

Supplemental Figure 2

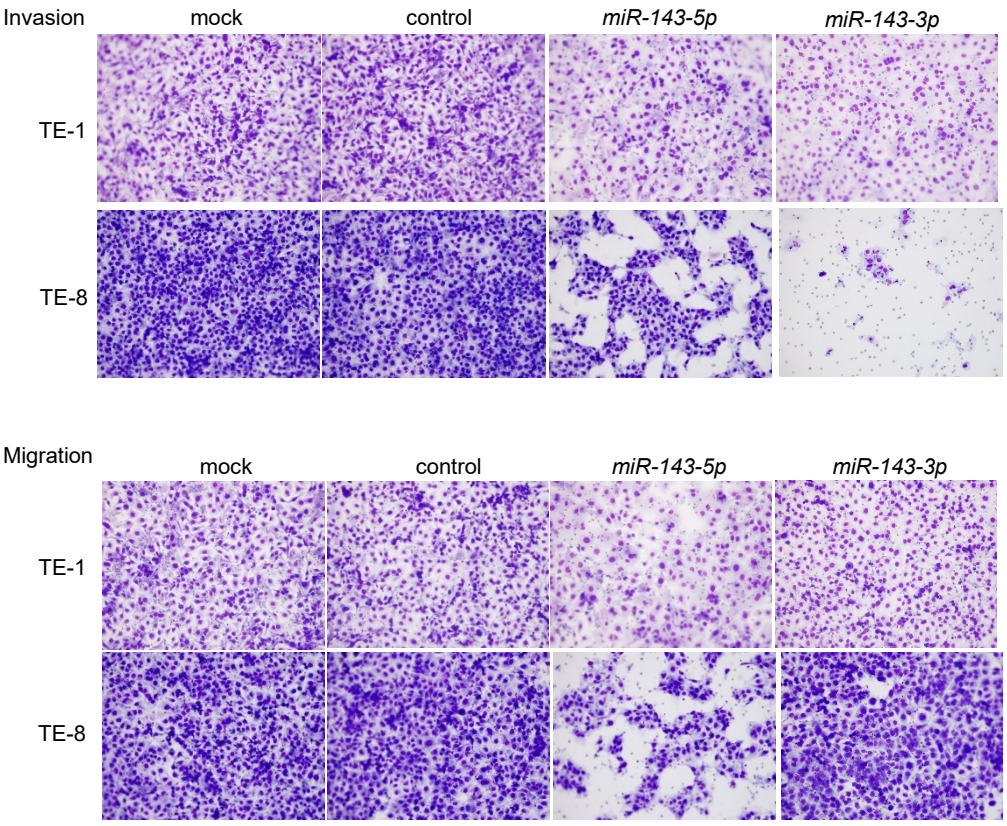

Supplementary Figure 3A

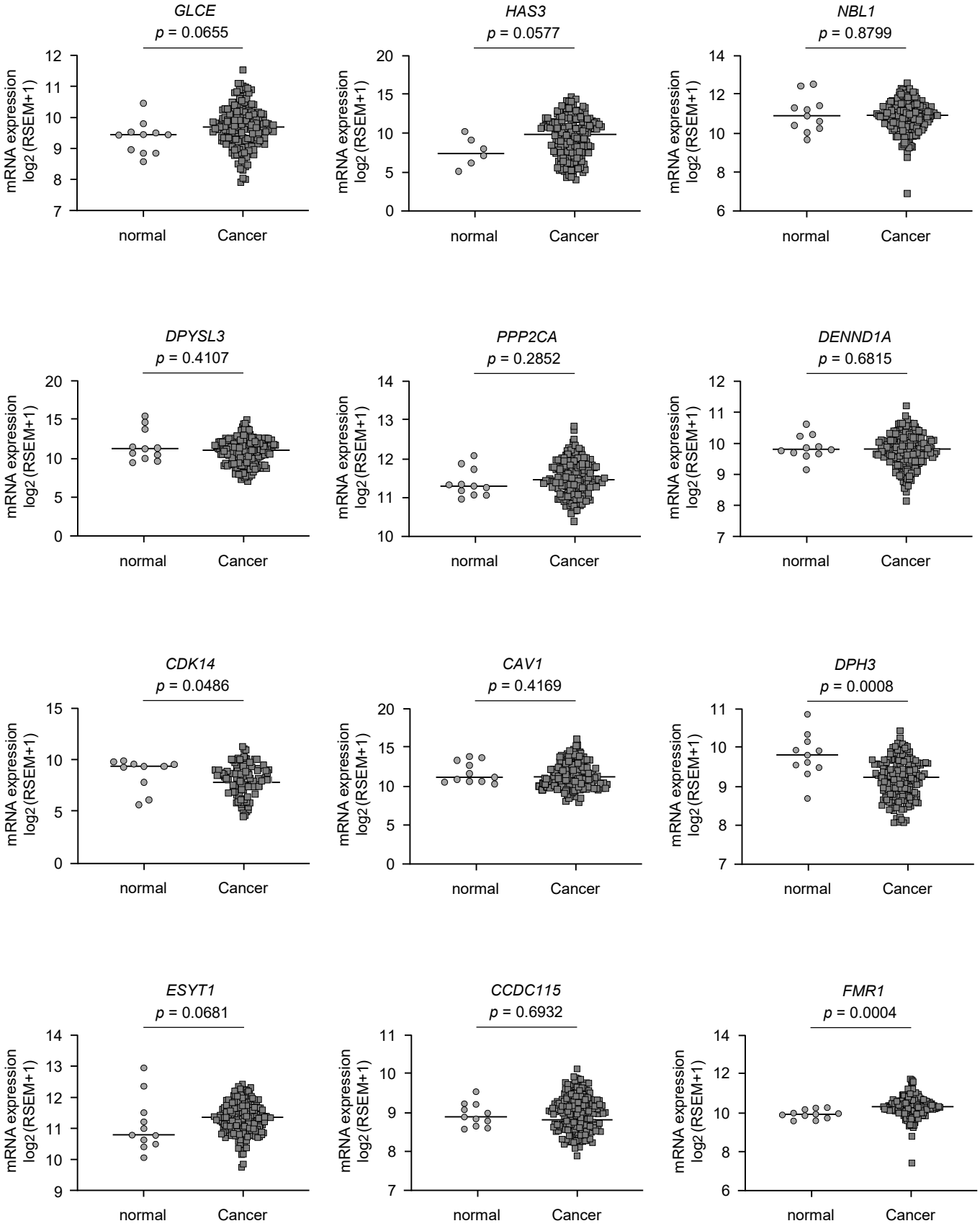

Supplementary Figure 3B

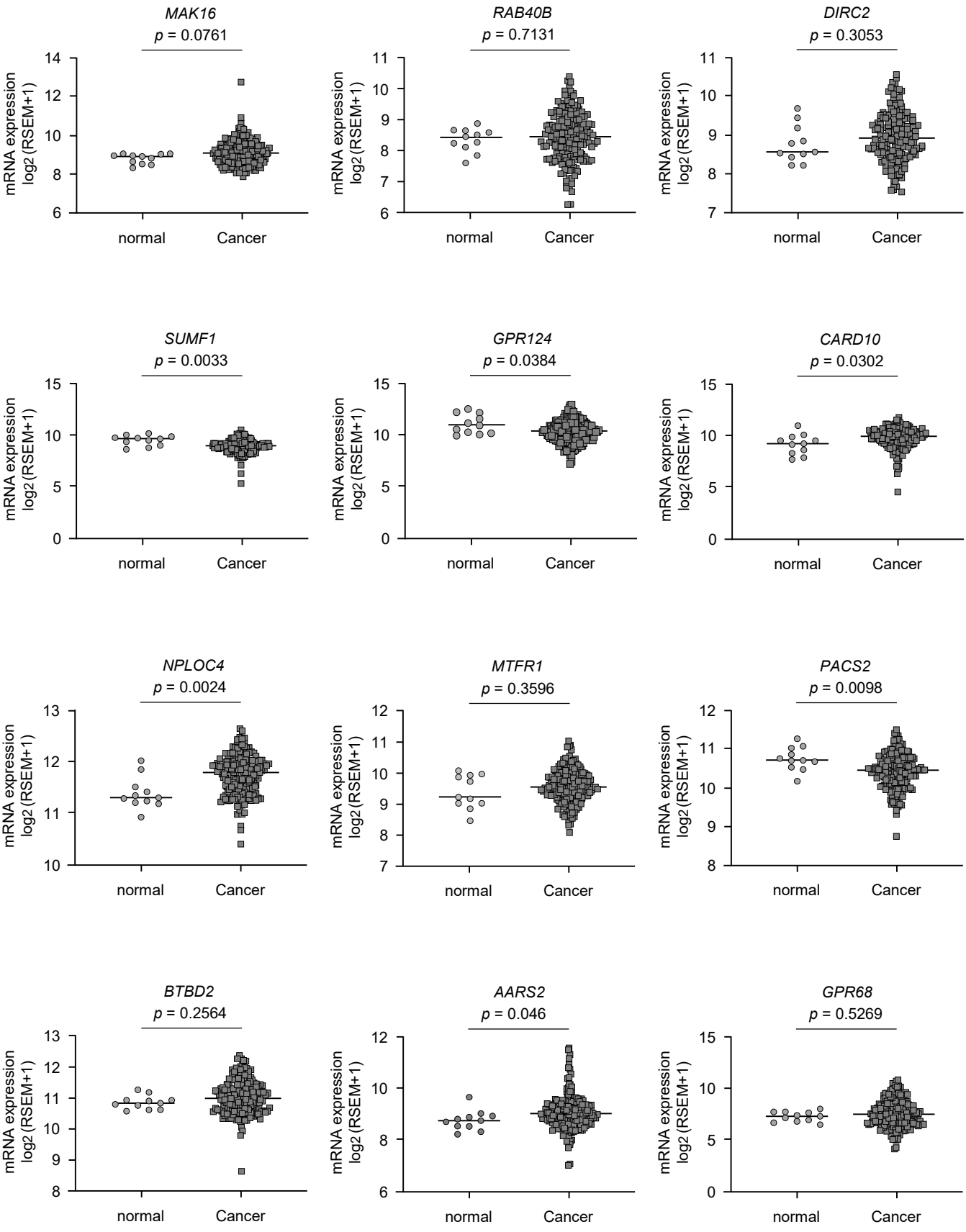

Supplementary Figure 3C

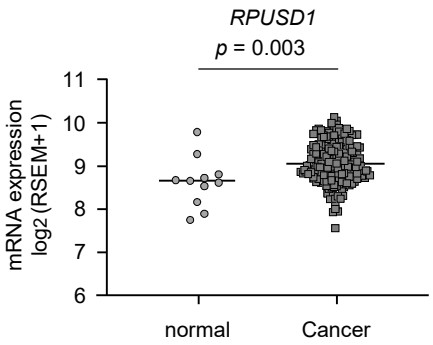

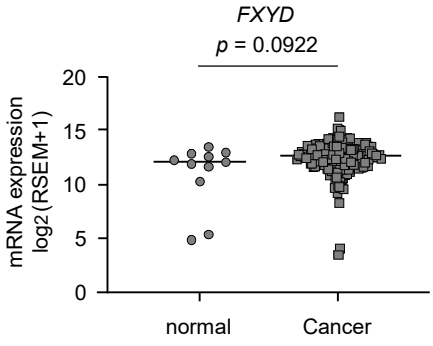

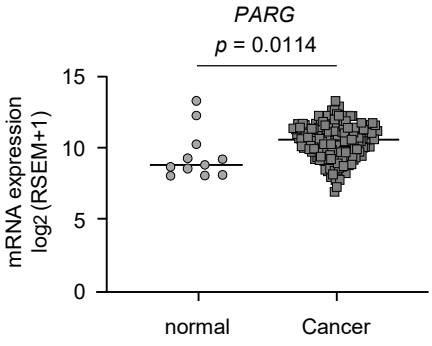

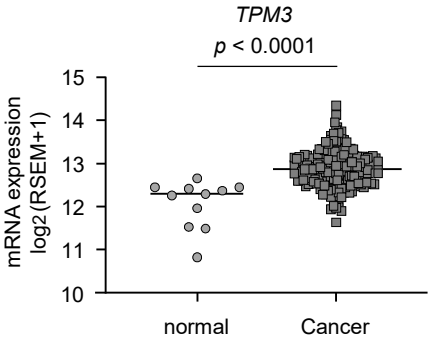

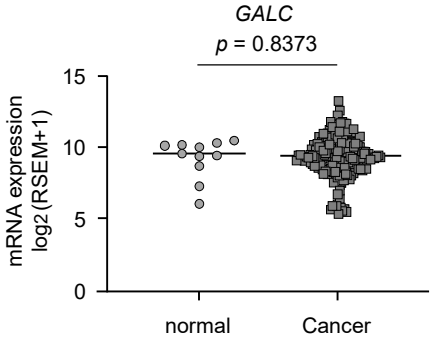

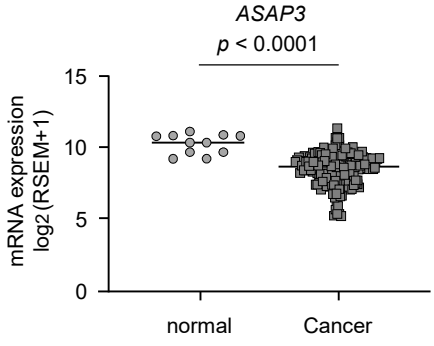

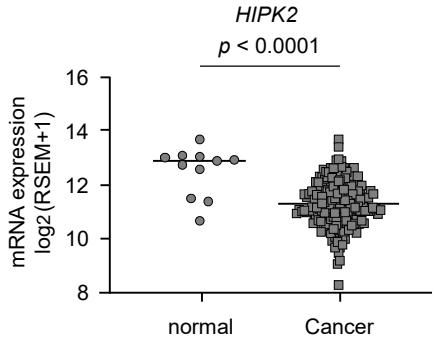

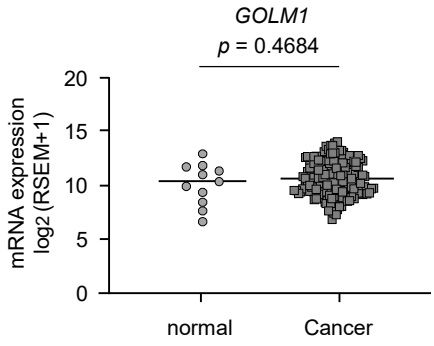

Supplementary Figure 4

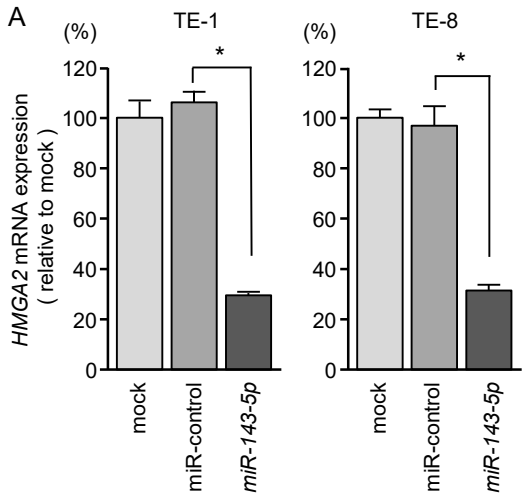

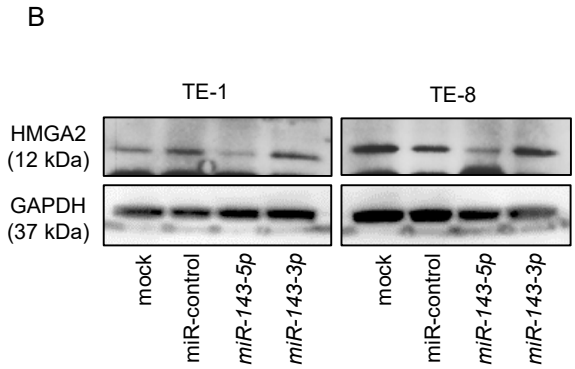

Position 371-377 of *HMGA2* 3'UTR

C

```
5′…UGGGUUUAGUCAAUCACUGCACU…3′ Wild type
3′  UGGUCUCUACGUCGUGACGCGG 5′ miR-143-5p
5′…UGGGUUUAGUCAAUC-------U…3′ Deletion type
```

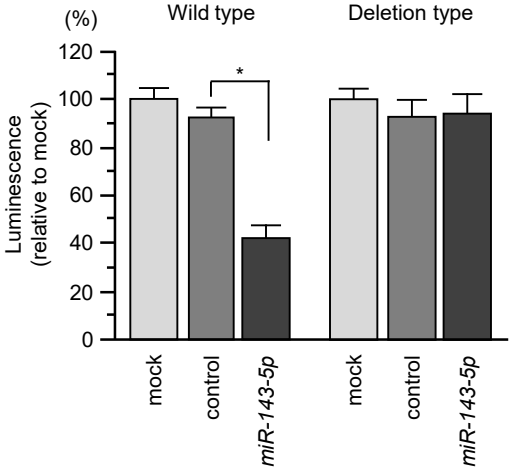

Position 1211-1217 of *HMGA2* 3'UTR

D

```
5′…CAUCUCUUCAUUCAAACUGCACU…3′ Wild type
3′  UGGUCUCUACGUCGUGACGCGG 5′ miR-143-5p
5′…CAUCUCUUCAUUCAA-------G…3′ Deletion type
```

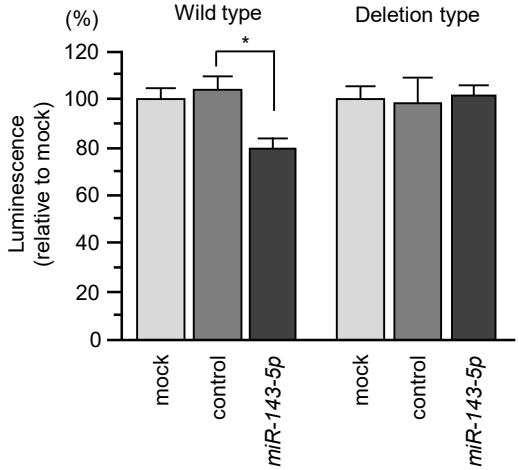

Position 2899-2905 of *HMGA2* 3'UTR

E

```
5′…UUAUCACUGUCUGUUCUGCACAA…3′ Wild type
3′ UGGUCUCUACGUCGUGACGUGG 5′  miR-143-5p
5′…UUAUCACUGUCUGUU-------A…3′ Deletion type
```

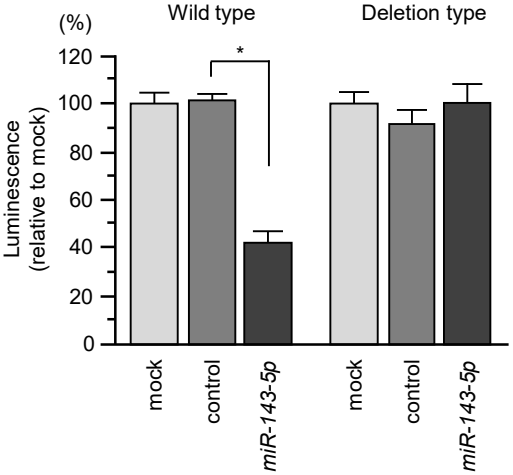

Supplemental Figure 4; WB full image of Supplemental Figure 4

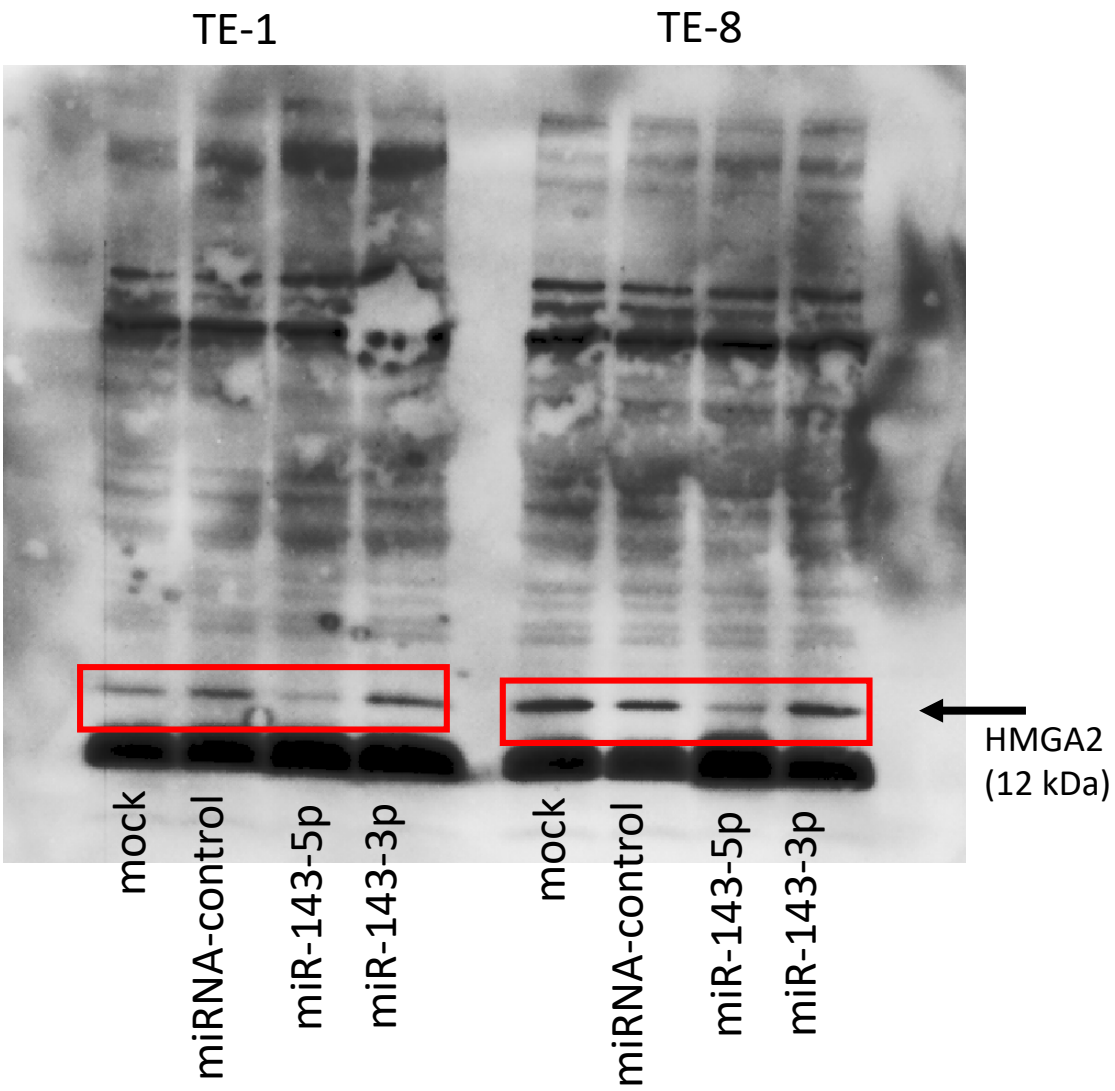

Supplementary Figure 5

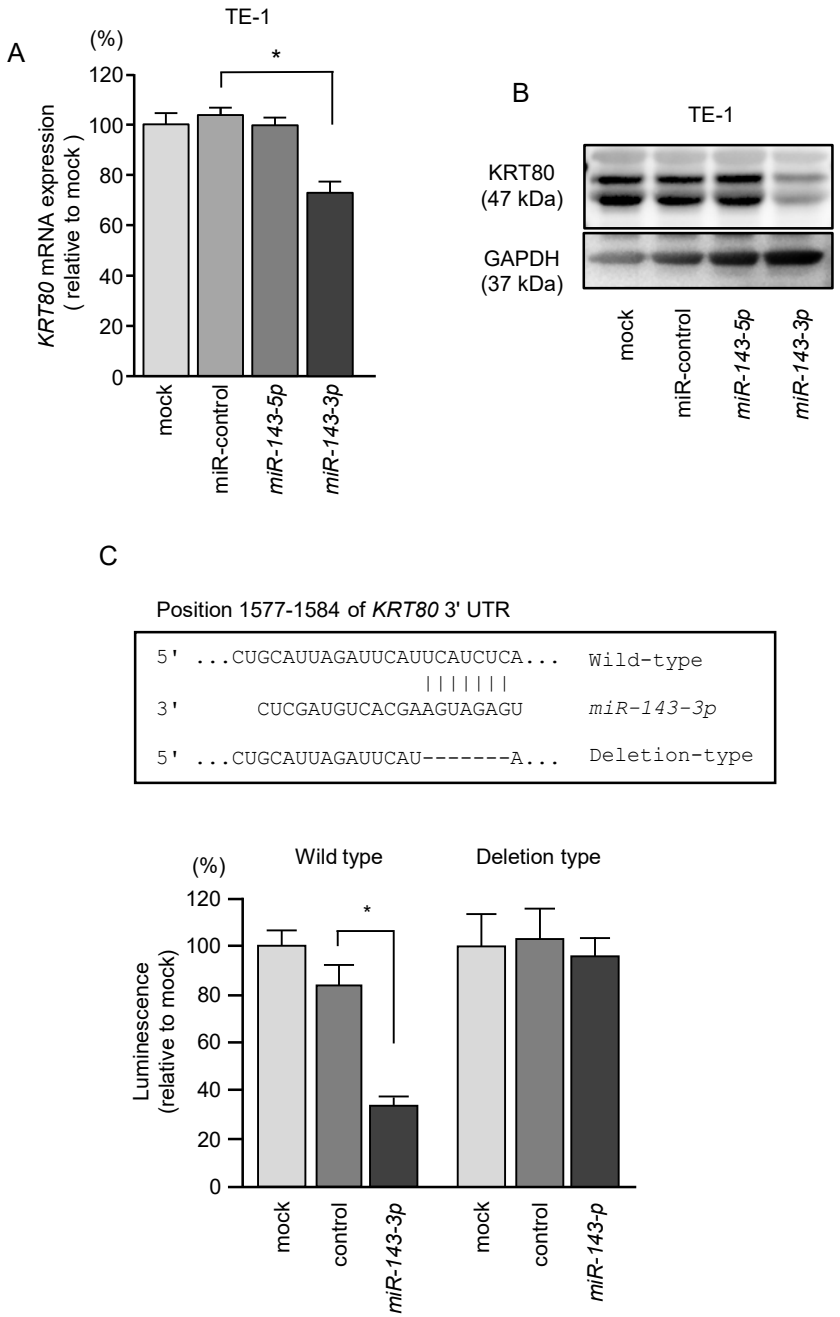

Supplemental Figure 5; WB full image of Supplemental Figure 5

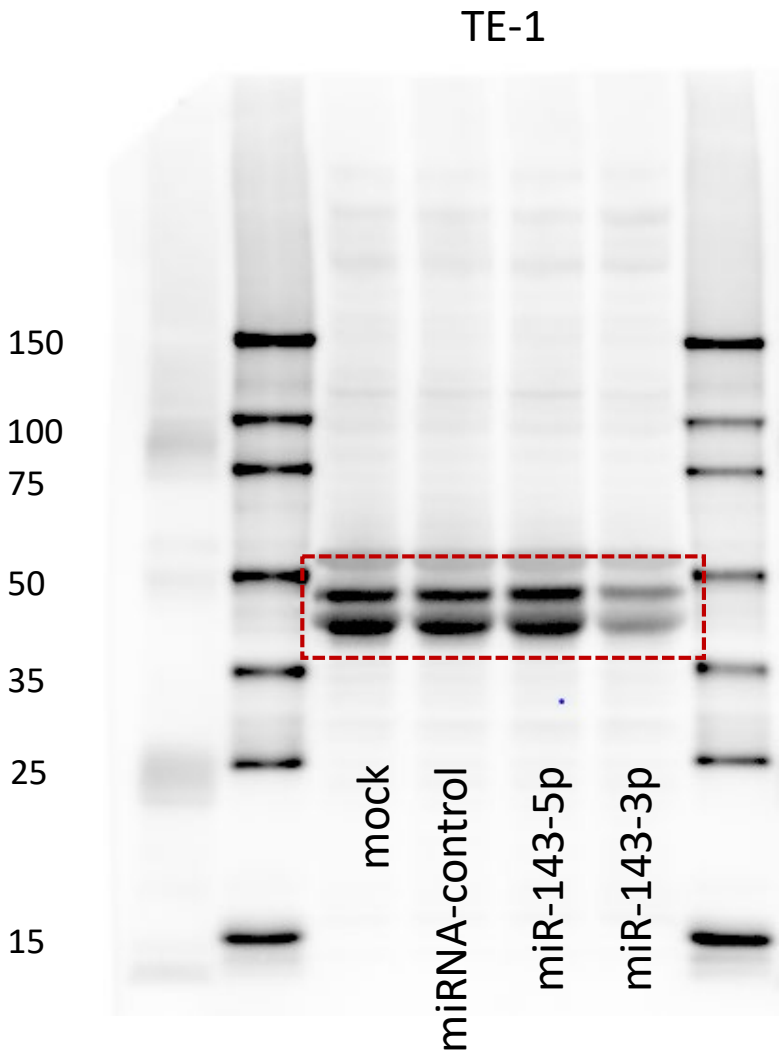

Supplemental Figure 6

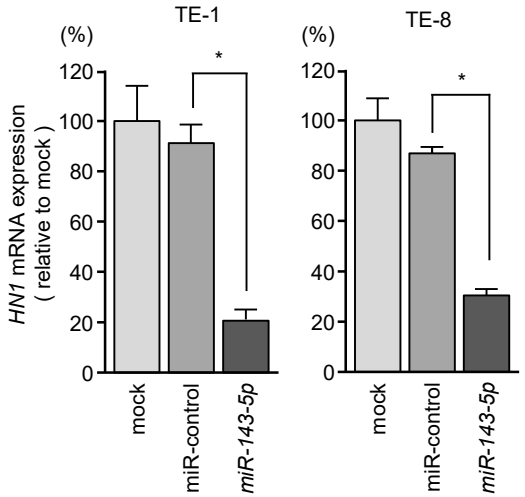

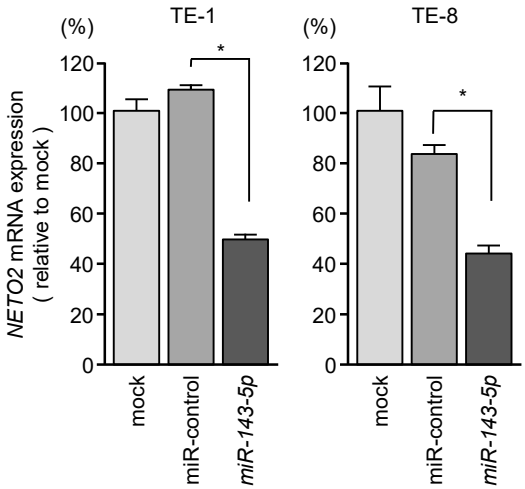

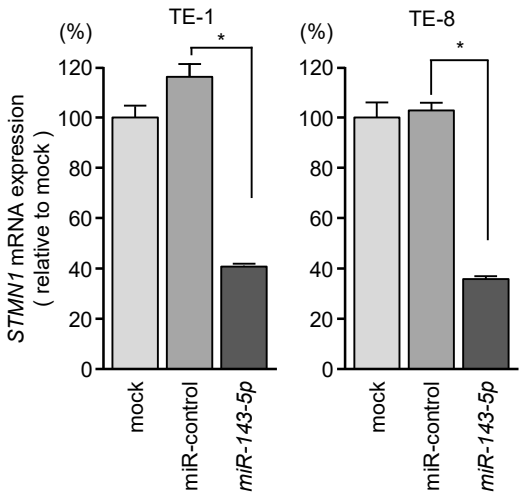

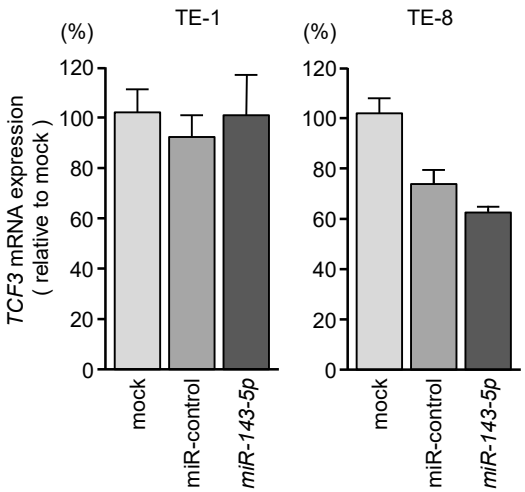

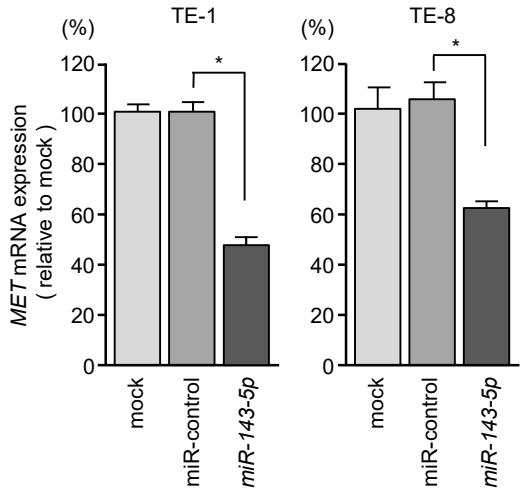

Supplemental Figure 7

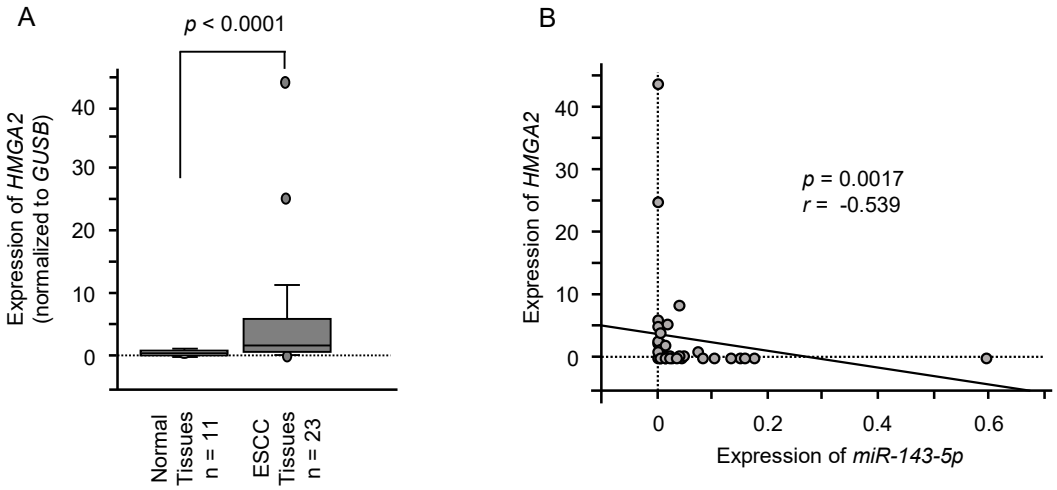

Supplemental Figure 8: Figure 4B WB full image

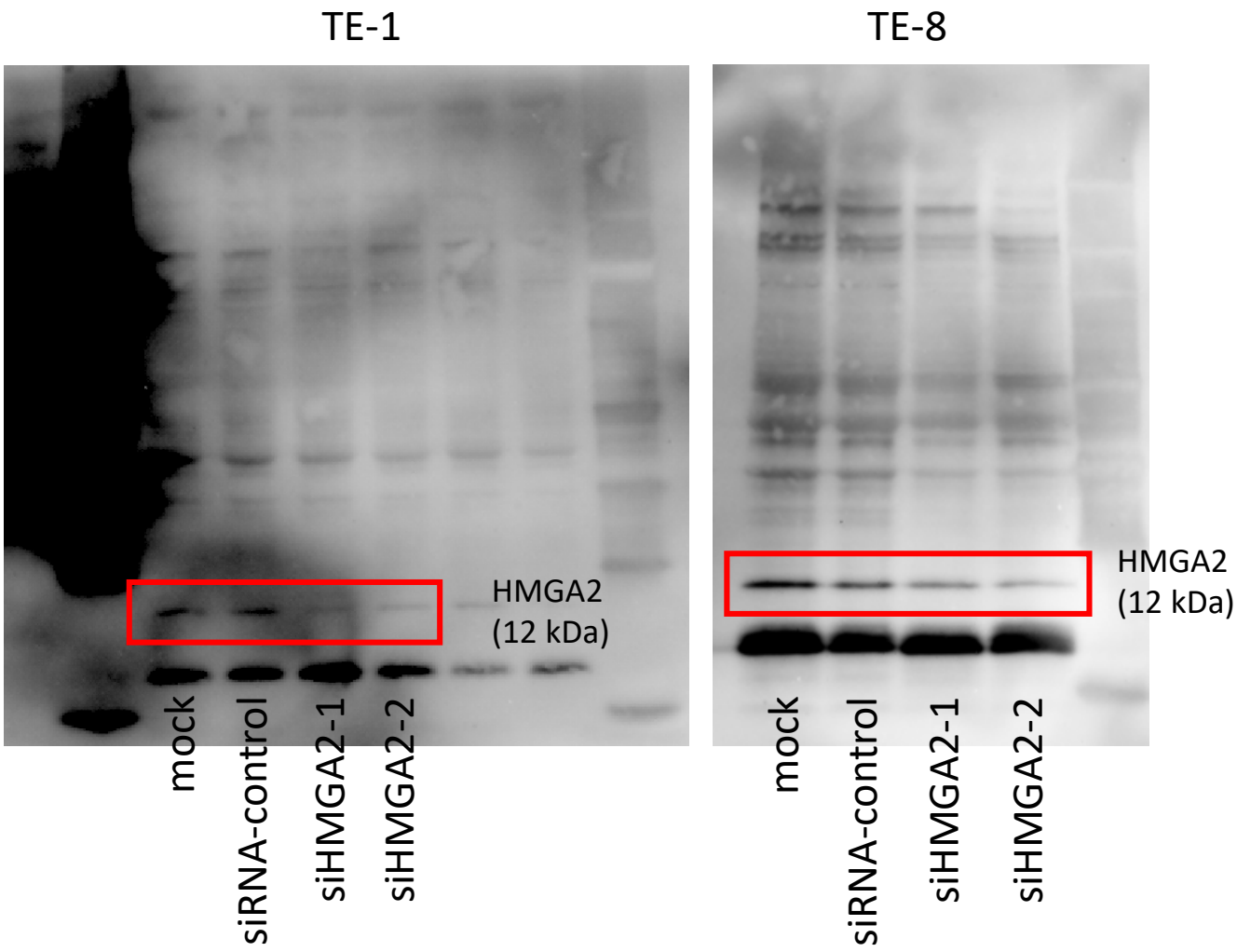

Supplemental Figure 9: Figure 4G WB full image